Energy & Environmental Science

ROYAL SOCIETY OF CHEMISTRY

REVIEW

View Article Online
View Journal | View Issue

Cite this: *Energy Environ. Sci.*, 2024, **17**, 7543

Safety concerns in solid-state lithium batteries: from materials to devices

Yang Luo,†[ab] Zhonghao Rao,†[a] Xiaofei Yang,[*bd] Changhong Wang,[c] Xueliang Sun[*c] and Xianfeng Li[*bd]

Received 30th May 2024,
Accepted 21st August 2024

DOI: 10.1039/d4ee02358g

rsc.li/ees

Solid-state lithium-metal batteries (SSLMBs) with high energy density and improved safety have been widely considered as ideal next-generation energy storage devices for long-range electric vehicles. Nevertheless, the potential safety issues in SSLMBs during solid-state electrolyte synthesis, battery operation and battery post-processing have been often ignored, which presents difficulties for their practical application. This review primarily evaluates the safety concerns in SSLMBs, especially thermal runaway and hazardous product release induced by the undesirable chemical/thermal/interfacial dynamic stability of the electrode and electrolyte materials. Subsequently, the recent advancements in addressing safety concerns by relying on electrolyte innovation and interface regulation as well as engineering SSLMB design are summarized, and future directions are speculated upon. The purpose of this review is to encourage researchers to devote more efforts to this field and pave the way for practical applications of SSLMBs.

Broader context

Ensuring both safety and high energy density is crucial for advancing energy storage technologies. Notably, the energy density of existing lithium-ion batteries is approaching its theoretical limit, and hence there is an urgent need to develop novel battery systems. In addition, flammable organic liquid electrolytes and their gaseous derivatives pose serious safety risks for batteries. Among various battery systems, solid-state Li metal batteries (SSLMBs) have emerged as promising candidates owing to their safety. Despite extensive research focused on enhancing ionic conductivity and optimizing electrode/electrolyte interfaces, recent studies have revealed unexpected safety issues, including thermal runaway events even in seemingly stable oxide-based SSLMB systems. Addressing these concerns is imperative for the continued progress of SSLMB technology. Herein, this review will comprehensively summarize the safety challenges of SSLMBs including the intrinsic stability of SSEs and the interfacial stability, as well as gas release. Corresponding strategies will be proposed *via* material design, battery operation, post-processing, *etc.*, to guide the future development and application of high-safety SSLMBs.

1. Introduction

As electric vehicles (EVs) rapidly develop, frequent safety incidents caused by thermal runaway and the demand for long ranges drive the development of the next generation batteries with high safety and high energy density. To date, conventional lithium-ion batteries (LIBs) hardly satisfy the above requirements due to their tricky safety concerns and limited energy density (<300 W h kg^{-1}).[1,2] Li metal batteries (LMBs) using the Li metal anode with high theoretical capacity (3860 mA h g^{-1}) and the lowest electrochemical potential (-3.04 V *vs.* standard hydrogen electrode) have attracted growing interest due to their higher energy density compared to state-of-the-art LIBs.[3] Nevertheless, the safety issues of LMBs including short circuits and thermal runaway still should be addressed.

Generally, the dendritic Li piercing the separator is the primary cause of short circuits. Furthermore, flammable organic liquid electrolytes and their gaseous derivatives are regarded as being responsible for violent burning or jet combustion.[4] Compared with liquid electrolytes, solid-state electrolytes (SSEs) possess obvious superiorities in many aspects, including (i) non-volatile nature and higher thermal stability, (ii) excellent mechanical strength to inhibit dendrite growth, and (iii) wider electrochemical stability windows and low reactivity, which allows for superior compatibility with

[a] *School of Energy and Environmental Engineering, Hebei University of Technology, Tianjin, 300401, China*
[b] *Dalian Institute of Chemical Physics, Chinese Academy of Sciences, Dalian 116023, China. E-mail: yangxf@dicp.ac.cn, lixianfeng@dicp.ac.cn*
[c] *Department of Mechanical and Materials Engineering, University of Western Ontario, London, Ontario, N6A 5B9, Canada. E-mail: xsun9@uwo.ca*
[d] *Laboratory of Advanced Spectro-Electrochemistry and Lithium-Ion Batteries, Dalian National Laboratory for Clean Energy, Dalian Institute of Chemical Physics, Chinese Academy of Sciences, Dalian 116023, China*
† Y. L. and Z. R. contributed equally to the work.

electrodes. Given the above virtues, SSEs offer a promising route for the implementation of Li anodes to achieve higher energy density and safer SSLMBs, making SSLMBs one of the most promising types of next-generation batteries.[5–7]

In the last few years, most of the efforts have been devoted to exploring high ionic conductors and solving the mismatched electrode/electrolyte interfaces, and eye-catching progress has been made. For instance, both sulfide and halide SSEs have achieved high ionic conductivities of over 10^{-2} S cm^{-1} that are comparable to those of liquid electrolytes.[8–11] More importantly, relying on structural innovation and interface decoration, the assembled SSLMBs have demonstrated an ultralong lifespan of over 10 000 cycles.[12,13] It seems that the practically accessible SSLMBs are near at hand. Nevertheless, very recently, some noteworthy exceptions contradicting the conventional "safe SSLMBs" concept have been reported. The thermal runaway was detected, even in highly stable oxide-based SSLMB systems.[14] Moreover, recent reports showed that solid polymer electrolytes (SPEs) and sulfide SSEs are also likely to react exothermically.[15–17] On grinding the sulfide SSEs (*e.g.* Li_3PS_4, $Li_7P_3S_{11}$) with Li or lithiated Si anodes, even in an inert atmosphere, an obvious combustion phenomenon was observed. When oxidation-state cathode materials were involved, the combustion reaction was more severe.[18] In other words, the risks of fire and explosion potentially exist in SSLMBs. These findings provoked us to think about whether SSLMBs are intrinsically safe.[14] Systematically pointing out the safety concerns and providing potential solutions are of significance to pave the way for practical application of SSLMBs.

In this review, as shown in Fig. 1, the safety concerns involved in material synthesis, battery operation and battery failure in SSLMBs will be first summarized. Furthermore, the unsafe factors including thermal runaway and hazardous product release induced by unstable SSEs, undesirable interfacial reactions, mismatched interface contact as well as uncontrollable Li dendrite growth will be deeply analyzed. Following that, potential solutions, mainly focused on electrolyte innovation and interfacial engineering design, will be discussed to improve the safety of SSLMBs. Then, advanced characterization techniques and theoretical calculations are systematically reviewed to

Yang Luo

Dr Yang Luo is currently a lecturer at the Hebei University of Technology. She received her BE degree from Southwest University in 2017 and PhD degree from Dalian Institute of Chemical Physics, Chinese Academy of Science (CAS), in 2022. Her research interests are focused on high-energy-density lithium metal batteries and electrochemical energy storage.

Zhonghao Rao

Prof. Zhonghao Rao is currently the Dean of the School of Energy and Environmental Engineering at Hebei University of Technology and the Director of the Hebei Engineering Research Centre for Advanced Energy Storage Technology and Equipment. He received his PhD degree from South China University of Technology in 2013 and joined Hebei University of Technology after working at China University of Mining and Technology for 8 years. His main research interest is battery thermal management.

Xiaofei Yang

Prof. Xiaofei Yang received his PhD degree in chemical engineering in 2018 from Dalian Institute of Chemical Physics (DICP), Chinese Academy of Sciences (CAS). After 3 years' postdoctoral work at Western University, he joined DICP in 2021. His research interests include Li–S batteries, all-solid-state lithium batteries, and battery interface studies via synchrotron X-ray characterization.

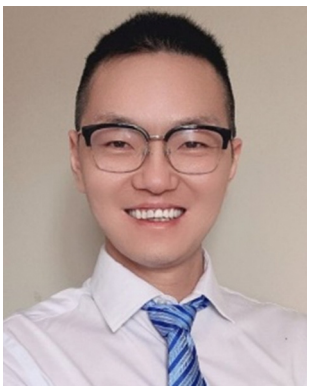

Changhong Wang

Dr Changhong Wang is currently a tenure-track Assistant Professor at Eastern Institute of Technology (EITech), Ningbo. He received his MS degree in material engineering from the University of Science and Technology of China in 2014 and PhD in mechanical and material engineering from the University of Western Ontario in 2020. His current research interests include all-solid-state batteries, solid electrolytes, lithium–sulfur batteries, and solid-state pouch cells.

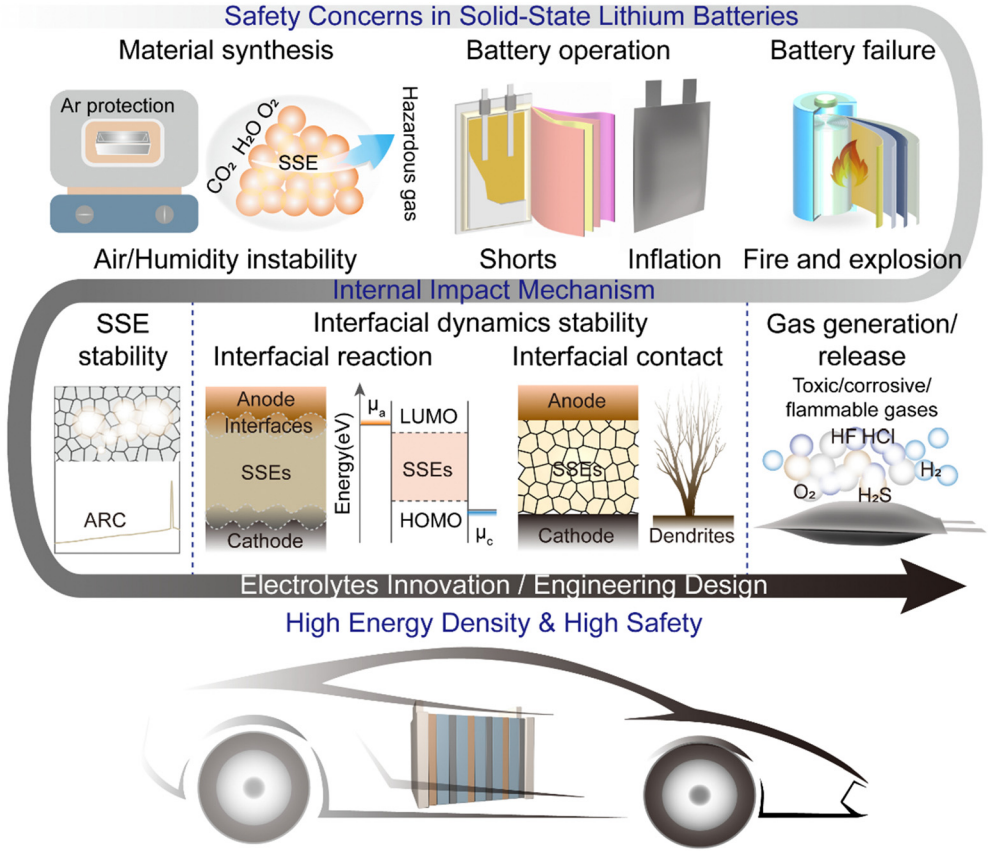

Fig. 1 Schematic representation of challenges for SSLMBs.

create a toolbox to understand battery failure mechanisms in terms of their heat evolution, dendrite growth, and gas emission. Finally, the rational design of practically accessible SSLMBs from the viewpoint of engineering (*e.g.*, building

Xueliang Sun

Prof. Xueliang Sun is a Foreign Fellow of the Chinese Academy of Engineering, a Fellow of the Royal Society of Canada and Canadian Academy of Engineering, and Chair Professor of the Institute of Materials and Energy at the Eastern Institute of Technology (tentative name), Ningbo, China. He served as Distinguished Professor at the University of Western Ontario and Chief Scientist in the Field of Nanoenergy Materialse, Canada. Dr Sun received his PhD in materials chemistry in 1999 from the University of Manchester, UK, following which he worked as a postdoctoral fellow at the University of British Columbia, Canada, and as a Research Associate at L'Institut National de la Recherche Scientifique (INRS), Canada. His current research interests are focused on advanced materials for electrochemical energy storage and conversion.

Xianfeng Li

Prof. Xianfeng Li is the Head of the Energy Storage Technology Research Department and Deputy Director of Dalian Institute of Chemical Physics (DICP), Chinese Academy of Sciences. Prof. Li received his PhD in polymer chemistry in 2006 from Jilin University. After 3 years' postdoctoral work at KU Leuven University, he joined DICP in 2009. His research interests mainly focus on electrochemical energy storage.

battery safety management systems and safe battery post-processing routes) will be discussed and the future directions will be speculated upon.

2. Safety challenges of SSLMBs

Conventional liquid electrolytes show poor safety performance owing to their flammability and reactivity. To address the safety concerns, SSLMBs using SSEs, especially inorganic solid electrolytes, are developed due to the theoretical nonflammability of SSEs. Nevertheless, recent studies have found that even solid-state lithium batteries suffer from severe exothermic reactions, which seriously affect battery safety.

Generally speaking, attention should be paid to the following processes, which seriously affect the safety of SSLMBs. (1) Intrinsic thermal/chemical stability of materials during preparation. (2) Interfacial dynamics processes during battery operation, including interfacial reactions and their products, as well as dendrite growth issues. Special attention should be paid to the heat accumulation and hazard release caused by the ohmic heat and internal reactions of cells during cycling. With this in mind, the intrinsic stability of SSEs and their compatibility with electrodes are particularly important. (3) The overlooked potential safety hazard of failed SSLMBs, *i.e.* the handling of harmful gases and the subsequent reaction of ruptured batteries should also be emphasized. In the following sections, we will evaluate the safety of SSLMBs by taking the intrinsic stability of SSEs and the interfacial stability as well as gas release into consideration.

2.1. Intrinsic instability of SSEs

The electrochemical performance and safety of SSLMBs are highly dependent on the intrinsic stability of SSEs. Notably, inorganic solid electrolytes such as sulfides and halides are reported to be sensitive to humidity, while SPEs exhibit poorer thermal stability compared with inorganic solid electrolytes. The intrinsic instability of SSEs would cause decomposition of SSEs as well as hazard release, limiting the safety and electrochemical performance improvement. Thus, the chemical and thermal stability of SSEs will be evaluated below.

2.1.1. Chemical instability. As described in Fig. 2a, inorganic solid electrolytes are considered highly sensitive to the ambient atmosphere, especially to moisture. Here the chemical reactions between inorganic solid electrolytes and the atmosphere, as well as the effect of the side products, are summarized according to the category of inorganic solid electrolyte (Fig. 2d). (1) Oxide SSEs. Oxide SSEs are considered one of the most stable inorganic solid electrolytes. Nevertheless, partial

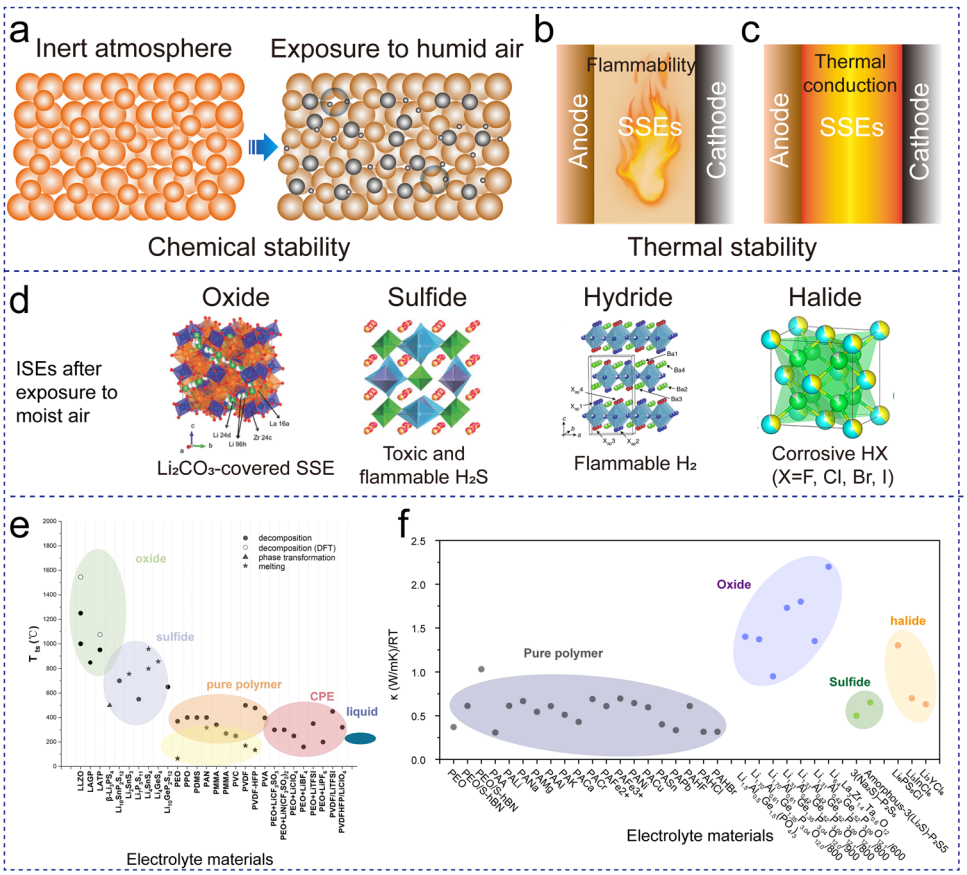

Fig. 2 (a)–(c) Factors affecting the thermodynamic stability of SSEs. (d) Chemical reaction mechanisms of several typical SSEs.[19,26,27] (e) The upper limit temperature of thermal stability of different SSEs. Reproduced with permission from ref. 28. (f) Thermal conductivity of different SSEs. Reproduced with permission from ref. 29.

oxide SSEs could react with CO_2 and H_2O in the humid atmosphere. Taking garnet-based SSEs ($Li_5La_3M_2O_{12}$ (M = Zr, Sn, Nb, and Ta)) as examples, they will react with H_2O and CO_2 to form LiOH and Li_2CO_3 on the surface, resulting in increased interfacial resistance, lower ionic conductivity and even more serious Li dendrite penetration.[19] (2) Sulfide SSEs. Compared with oxide SSEs, sulfide SSEs are more sensitive to O_2 and H_2O, where the PS_4^{3-} tetrahedra may react with H_2O to release toxic H_2S gas.[20–22] (3) Hydride SSEs. Similar to sulfide SSEs, hydride SSEs face the challenge of humidity stability as well. Taking $LiBH_4$ as an example, $LiBH_4$ will decompose in the presence of moisture to release H_2 gas, which is considered highly flammable and may burn at a low concentration.[23] (4) Halide SSEs. Compared with sulfide and hydride SSEs, halide SSEs are moderately air-stable. However, it is still highly recommended that halide SSEs should be handled in a dry environment, especially the strongly hygroscopic chlorides and bromides. For instance, Li_3InCl_6 will react with H_2O to form In_2O_3, LiCl and HCl after long-term exposure to humid air. HCl presents high corrosiveness, which would contribute to the corrosion of the current collector and human body.[24,25] Meanwhile, recently reported Li-compatible $Li_9N_2Cl_3$ presents similar properties to Li_3N with high reductivity, which is speculated to be sensitive to humidity, generate NH_3 and cause safety concerns as well.[26]

In summary, almost all inorganic solid electrolytes are unstable in moist air. In terms of SSE reactivity and their decomposition products, the chemical stability of SSEs may be in the following order: oxides > halides > sulfides > hydrides. By-products such as H_2S, H_2, NH_3 and HX (X = F, Cl, Br, I) when inorganic solid electrolytes are exposed to humid air will induce unsafe factors during large-scale production. Thus, appropriate synthesis approaches and stabilization strategies for SSEs as well as specific handling conditions should be considered during the synthesis process.

2.1.2. Thermodynamic instability. In the former section, the chemical reactions between inorganic solid electrolytes and the humid air, as well as the potential risks caused by the by-products were summarized. To our knowledge, in addition to chemical instability, the thermal stability of SSEs, including thermal decomposition temperature and thermal conductivity (Fig. 2b and c), is another consideration to evaluate the safety of the assembled SSLMBs, especially during the SSLMB operation. In the evaluation of the thermal stability of SSEs, T_{ts} defined as the decomposition temperature or the high-impedance phase transformation temperature, is used. Based on available research, as shown in Fig. 2e, the order of thermal stability is oxide SSEs > sulfide SSEs > SPEs > liquid electrolytes.[28] It could be seen that compared with SPEs, inorganic solid electrolytes exhibit higher thermal stability (T_{ts} > 400 °C) which is attributed to their stable lattice structures. To deeply understand the impact of lattice structure on thermal stability, a new thermal stability parameter Th was proposed to calculate and predict the essential thermal stability of inorganic solid electrolytes. The research found that Th is highly related to the crystal structure, polyhedral configuration, bond energy, bond type, bond number, normalization factor, *etc.*[30] Taking typical sulfide electrolytes as an example, relying on the theoretical prediction, the thermal stability order follows Li_6PS_5Cl > Li_4SnS_4 > $Li_{9.54}Si_{1.74}P_{1.44}S_{11.7}Cl_{0.3}$ > Li_3PS_4 > $Li_7P_3S_{11}$, which coincides well with the experimental results.

For SPEs, the thermal stability of the polymer matrix is mainly affected by the chemical structure of the polymer monomer, degree of polymerization, length of the polymerization segment, and degree of crystallization. Taking polyethylene oxide (PEO) as an example, polymer chain segments may break and form small molecular compounds or gaseous products when reacted with the Li anode or under elevated temperature. Therefore, designing stable chain segment structures is beneficial for improving the chemical/thermal stability of SPEs. Apart from the polymer matrix, Li salts and additives are the main components of SPEs, which also directly affect the overall thermal stability of SPEs from the perspectives of their decomposition temperature and interactions with polymers.[31] Abels *et al.* investigated the effect of several commonly used Li salts on the thermal stability of PEO.[31] The results showed that $LiClO_4$ accelerated PEO decomposition and showed strong exothermic combustion around 347 °C. In contrast, lithium bis(trifluoromethanesulfonyl)imide (LiTFSI) and lithium bis(pentafluoroethanesulfonyl)imide (LiBETI) had a negligible effect on PEO decomposition, where PEO decomposed at roughly 400 °C. Therefore, LiTFSI and LiBETI are much more appropriate in terms of safety than $LiClO_4$. Apart from Li salts, introducing flame retardants (*e.g.* halogen, phosphorus and nitrogen-based flame retardants) as additives can effectively inhibit SPE combustion. Generally, flame retardants play the following two roles in improving the safety of SPE-based SSLMBs: (1) promoting the dehydration and carbonization of polymer materials, and preventing flammable gases from releasing and (2) forming a protective film to isolate the outside air and heat. Among them, organophosphorus-based flame retardants (phosphates, phosphites, phosphonates, phosphazenes, *etc.*) are widely adopted due to their low toxicity and high flame retarding efficiency.[32]

Besides the intrinsic thermal stability, the thermal conductivity of SSEs also affects the temperature distribution inside SSLMBs. The electrochemical reaction accompanied by heat release affects the internal temperature distribution of SSLMBs, and *vice versa*. More seriously, massive heat accumulation may cause thermal runaway of SSLMBs; however it has received little attention. Recently, the thermal conductivity (k) of SSEs was systematically studied.[29] As described in Fig. 2f, oxide SSEs possess higher k (1–2.2 W m^{-1} K^{-1}) than SPEs (0.2–0.7 W m^{-1} K^{-1}), which facilitates the uniform distribution and conduction of heat and prevents SSLMBs from heating up drastically due to heat accumulation. Nevertheless, the high thermal conductivity of SSEs can't totally ensure superior internal heat transfer. Recent research studies have shown that the main thermal resistance of batteries is derived from the interfacial thermal resistance; thus reducing the interfacial thermal resistance is of great significance for enhancing the internal heat transport performance of batteries.[33]

2.2. Interfacial dynamic instability

As mentioned above, the intrinsic stability of SSEs can't represent the thermal stability of SSLMBs, and in actual situations, the electrode/SSE interface usually exhibits different chemical/dynamic/thermal behavior compared with either electrodes or SSEs. The Li plating/stripping process is accompanied by interface dynamics variations including the interfacial reaction products, physical contact, Li deposition morphology and temperature distribution, which also affect the safety of SSLMBs.

2.2.1. Interfacial side reactions. Understanding the interface is important, as it provides critical information on the interfacial reaction and the electrochemical performance of SSLMBs. As shown in Fig. 3a, the chemical stability of SSEs is determined by the energy separation between the lowest unoccupied molecular orbital (LUMO) and the highest occupied molecular orbital (HOMO).[34] Typically, a higher LUMO energy reflects higher anti-reduction, while a higher HOMO energy represents better anti-oxidation. In the current research stage, none of the SSEs can match both cathode materials and anode materials concurrently with wide electrochemical stability windows beyond 0–5 V. Thus, in most cases, the SSEs would react with anode or cathode materials to form interface layers, either solid electrolyte interphase (SEI) or cathode electrolyte interphase (CEI). Generally, interfaces between SSEs and electrodes are primarily classified into three categories: (I) thermodynamically stable interfaces; (II) mixed electronic-ionic conducting interfaces (MCI); and (III) ion-conducting interfaces with negligible electronic conductivity. Only type I (stable) and type III (passivated) interfaces ensure stable long-term SSLMBs.[35] Type I exists in ideal inert SSEs that are compatible with both cathodes and anodes. Type III is an ideal interface to inhibit continuous side reactions. Unfortunately, almost all recently reported SSEs tend to continuously react with either Li metal or the highly charged state cathodes, resulting in capacity decay and safety concerns. Therefore, it is essential to modulate the interfacial reaction, in turn, to regulate reactivity and ion transport at the interfaces, ultimately improving the performance of SSLMBs.

Despite the tremendous efforts in studying electrode/SSE interfaces, reports on interface security hazards are rare to date. Several factors related to interfacial stability, including material compatibility, heat accumulation, and gas release, should be considered when designing high-safety SSLMBs.

(1) Li/SSE interfacial reactions. Recent reports showed that the exothermic reaction of SSEs and Li metal will affect Li deposition behavior and the stability of SSEs. On one side, high-valence-metal-element-containing SSEs such as $Li_{10}GeP_2S_{12}$ (LGPS), $Li_{1+x}Al_xGe_{2-x}(PO_4)_3$ (LAGP), and $Li_{1+x}Al_xTi_{2-x}(PO_4)_3$ (LATP) will be reduced by Li metal to form an unstable MCI. The MCI enables the continuous decomposition of SSEs and increased interfacial resistance. The electrical properties of the interphase strongly affect the mechanical integrity of LAGP. The MCI forces Li^+ reduction at the LAGP side rather than the Li side, causing a local volume expansion, crack formation and the pulverization of LAGP. Furthermore, interfacial reactions are usually accompanied by heat generation. When MCI reacts dramatically with melted Li when the temperature is over 200 °C, the thermal runaway occurs.[36] To further reveal the failure mechanism of oxide SSEs, multiscale characterization was employed to study the thermal reaction of LATP and Li.[37] It was found that LATP would react with Li to form Li_3PO_4, LiP, $Li_{0.5}TiO_2$, *etc.*, at elevated temperatures and release a large amount of heat. Besides, molten Li

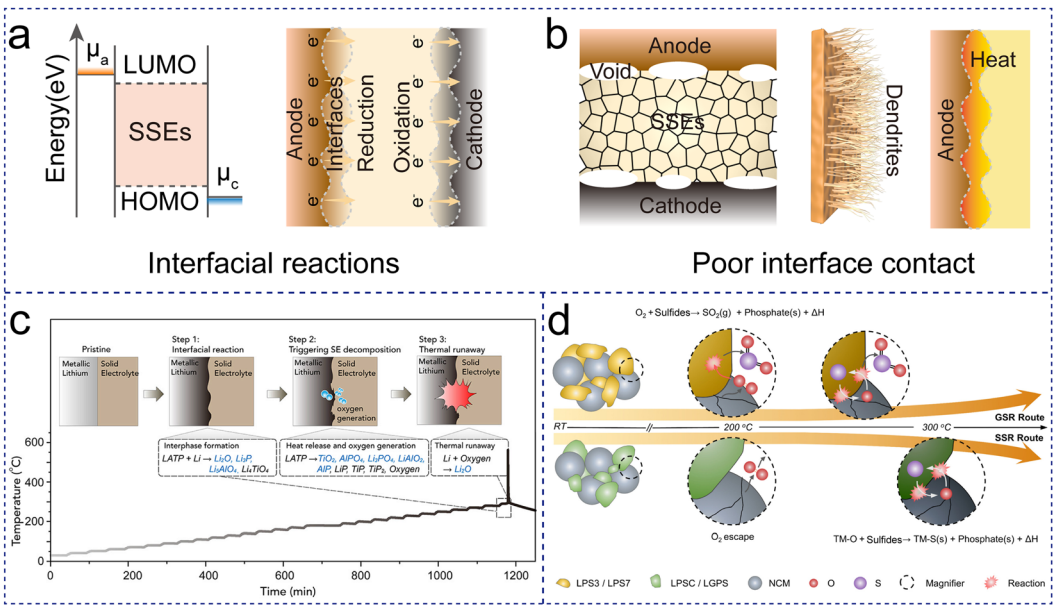

Fig. 3 Interfacial dynamic instability of SSLMBs. (a) Interfacial reaction mechanisms of SSEs. (b) The issues caused by mismatched interfacial physical contact. (c) Scheme of multi-step thermal runaway reaction between oxide SSEs and Li metal. Reproduced with permission from ref. 14. (d) Schematic diagram of the two distinct failure routes of different sulfide SSEs with NCM. Reproduced with permission from ref. 17.

diffuses along the microcracks of LATP and its products, intensifying the thermal reaction with LATP, and causing thermal runaway for LATP. In another case, it was found that O_2 is another by-product of the interfacial reactions of Li and LATP, where O_2 participated in the subsequent reaction with molten Li to induce thermal runaway (Fig. 3c).[14] These results suggested that even high-stability SSEs are threatened by interfacial decomposition products, which reminds one to reconsider the fundamental interfacial safety issues of SSLMBs.

(2) Cathode/SSE interfacial reactions. In addition to the SSE/Li interface, safety concerns regarding the SSE/cathode interface should be considered. The electrochemical and thermodynamic instability is a hidden safety concern. For SPEs, their poor anti-oxidant properties cause incompatibility with high-voltage cathode materials, even releasing O_2, CO, C_2H_2, *etc*.[38] Additionally, some hydrocarbon polymers also face the risk of burning.[39,40] Taking PEO as an example, when matching to high voltage cathode materials, such as $LiCoO_2$ or $LiNi_xCo_yMn_{1-x-y}O_2$ (NCM), the $LiCoO_2$ surface will catalyze the PEO electrolyte to release unexpected H_2 gas,[38] and NCM may react with thermally degrading PEO or fluorine radicals (from lithium salts) to release O_2 and subsequently polymer combustion may occur, threatening battery safety.[31] Similarly, inorganic solid electrolytes also face the risk of gas production/heat accumulation from the reaction with cathode materials. Typically, sulfides are a class of SSEs with high ionic conductivity, while showing relatively poor electrochemical stability. Recently, Wang and co-authors explored the thermal stability of sulfide SSEs and the $Li_{1-x}CoO_2$ cathode at 400–500 °C.[18] It was found that Li_3PS_4 would decompose into reducible and flammable Li_2S and S. Such products may be in direct contact with $Li_{1-x}CoO_2$ and lead to an exothermic reaction or even combustion at a certain temperature. The interfacial stability of Li_3PS_4 and NCM was further estimated *via* differential thermal analysis (DTA) measurements, and the results showed exothermic peaks appearing at 340–420 °C, suggesting their lower thermal stability. Recent research found that the interfacial stability of cathode/SSE materials is highly dependent on the structure of SSE and cathode materials. For instance, when the P in Li_3PS_4 is totally substituted by Sn, the interfacial reactions are suppressed and no distinct exothermic peaks are observed in NCM–Li_4SnS_4. It can be attributed to the stronger Sn–S bond, where S is more difficult to be substituted by O (from NMC) compared with the P–S bond.[41]

Notably, the thermal safety of SSLMBs is threatened by lattice oxygen (O_2) release from cathodes. Recently, a new view reported that Li presented relatively high thermal stability against sulfide SSEs and O_2 under practical working conditions. It is confirmed that no thermal runaway was detected in an Ah-level Li|NCM pouch cell using the Li_6PS_5Cl electrolyte before charging. Nevertheless, when charging to 100% state-of-charge (SOC), there is intense exothermic heat generation due to the reaction of O_2 and Li_6PS_5Cl. After the temperature reached 275.5 °C, a short circuit occurred. Thus, inhibiting the release of lattice oxygen is important for enhancing the thermal stability of SSLMBs.[42] Furthermore, differential scanning calorimetry-mass spectrometry (DSC-MS) characterization is used to understand the thermal failure of the sulfide SSE and the NCM cathode. Here two distinct thermal runaway mechanisms of sulfide-based SSLMBs using glass-ceramic (Li_3PS_4 and $Li_7P_3S_{11}$) and crystalline (Li_6PS_5Cl and $Li_{10}GeP_{12}S_2$) sulfide SSEs were revealed, named the gas–solid and the solid–solid reactions (Fig. 3d).[17] The glassy-ceramic SSEs experienced a gas–solid reaction, which was oxidized by O_2 (released from NCM cathodes) at approximately 200 °C, leading to toxic SO_2 generation and tremendous heat. In contrast, the crystalline sulfide SSEs remained stable against lattice O_2 at 200 °C without SO_2 generation, while solid–solid reactions occurred with the decomposition products of NCM cathodes (transition-metal oxides, *etc.*) at 300 °C. The mechanism suggests that strategies such as inhibiting O_2 release from cathode materials and optimizing the crystal structure of SSEs facilitate achieving safer SSLMBs. In addition, cathode materials also play an important role in determining interfacial stability. Compared to layered metal oxide cathode materials, sulfide SSEs show better thermal stability towards $LiFePO_4$. Taking Li_6PS_5Cl as an example, it is thermally stable towards $LiFePO_4$ even at 350 °C. In contrast, Li_6PS_5Cl showed vigorous exothermic chemical reactions with delithiated $Li_{1-x}Ni_{0.8}Co_{0.1}Mn_{0.1}O_2$ (NCM811).[43] In short, the proposed mechanisms established the relationship among the sulfide SSE structures, gas-driven crosstalk reactions, and interfacial reactions during the thermal runaway, guiding the rational design of interfaces.

Compared with sulfide SSEs, halide SSEs possess better air stability and anti-oxidation, especially fluoride-based SSEs. However, their interfacial-level electrochemical/thermal stability is unclear. Recently, the interfacial thermal stability of halide SSEs and electrodes was explored, and it was confirmed that anti-perovskite-type Li_2OHCl was compatible with the cathode and anode at a relatively low temperature, while exhibiting high chemical reactivity after melting over 320 °C. In contrast, rock-salt-type Li_3InCl_6 showed higher thermal stability and interfacial compatibility.[44] Nevertheless, the oxidation by-products may contain toxic Cl_2 based on Mo's simulation for most chloride-based SSEs. In practical pouch cells, the sealing packages are easily blasted and result in the leakage of Cl_2, which increases safety risks.[45] As another important SSE with high stability against Li anode, hydride SSEs have also attracted great attention.[46] However, according to Lu's simulation, the hydride SSEs present poor oxidation stability. $LiBH_4$ and $Li_2B_{12}H_{12}$ would be oxidized into flammable H_2 under a voltage of ~2 V and ~3.3 V (*vs.* Li^+/Li), respectively, which poses potential hazards.[47]

As aforementioned, the structure of SSEs and their compatibility with anodes/cathodes have a significant effect on interfacial stability. More considerable efforts are required to study the interfacial stability mechanisms of SSEs and electrodes to guide the design of high-performance SSEs. More efforts are recommended to focus on exploring SSEs with wide electrochemical stability windows to match both cathode and anode materials.

2.2.2. Mismatched interfacial physical contact. Apart from interfacial reactions, the solid–solid interface between

electrodes and inorganic solid electrolytes should be taken into account (Fig. 3b). (1) Poor physical contact. "Solid–solid" ("point-to-point") physical contact mode between SSEs and active material particles slows down the Li^+ transport rate at the interface and causes huge interfacial impedance. Continuous volume changes and gas release further aggravate interfacial issues, resulting in fast capacity decay and even SSLMB failure.[48] (2) Dendrites. The growth of dendrites can be attributed to the Li^+ concentration gradient during plating, uneven Li^+ distribution at the interface, and uneven electrode surface. Besides, dendrites tend to grow along grain boundaries with a reduced band gap, where Li^+ is preferentially reduced by electrons to form local Li filaments and cause short circuits during cycling.[49] (3) Thermal distribution. The uneven distribution of hotspots at the interface will induce Li dendrite growth and thermal runaway. It was found that the LATP pellet, with rich defect sites (atomic structural defects, cracks, voids, *etc.*) and high reactivity, would lead to higher interfacial reactivity and earlier thermal runaway.[50] This is because metallic Li can penetrate the defect sites of the LATP bulk phase under elevated temperatures and result in the inferior thermal stability of the Li/LATP pellet. Thus, enhancing the compatibility and stability as well as reducing the defects of SSEs *via* interfacial engineering to improve interfacial contact, retard heat accumulation and prevent by-product formation is highly suggested.

2.3. Gas release

In addition to short circuits and heat accumulation, gas accumulation is another factor leading to battery failure. As mentioned in Sections 2.1 and 2.2, gases (such as O_2, H_2, HX, NH_3 and H_2S) are mainly derived from material preparation and battery operation processes (Fig. 4a). Firstly, these hazardous gases would cause environmental pollution and health hazards.

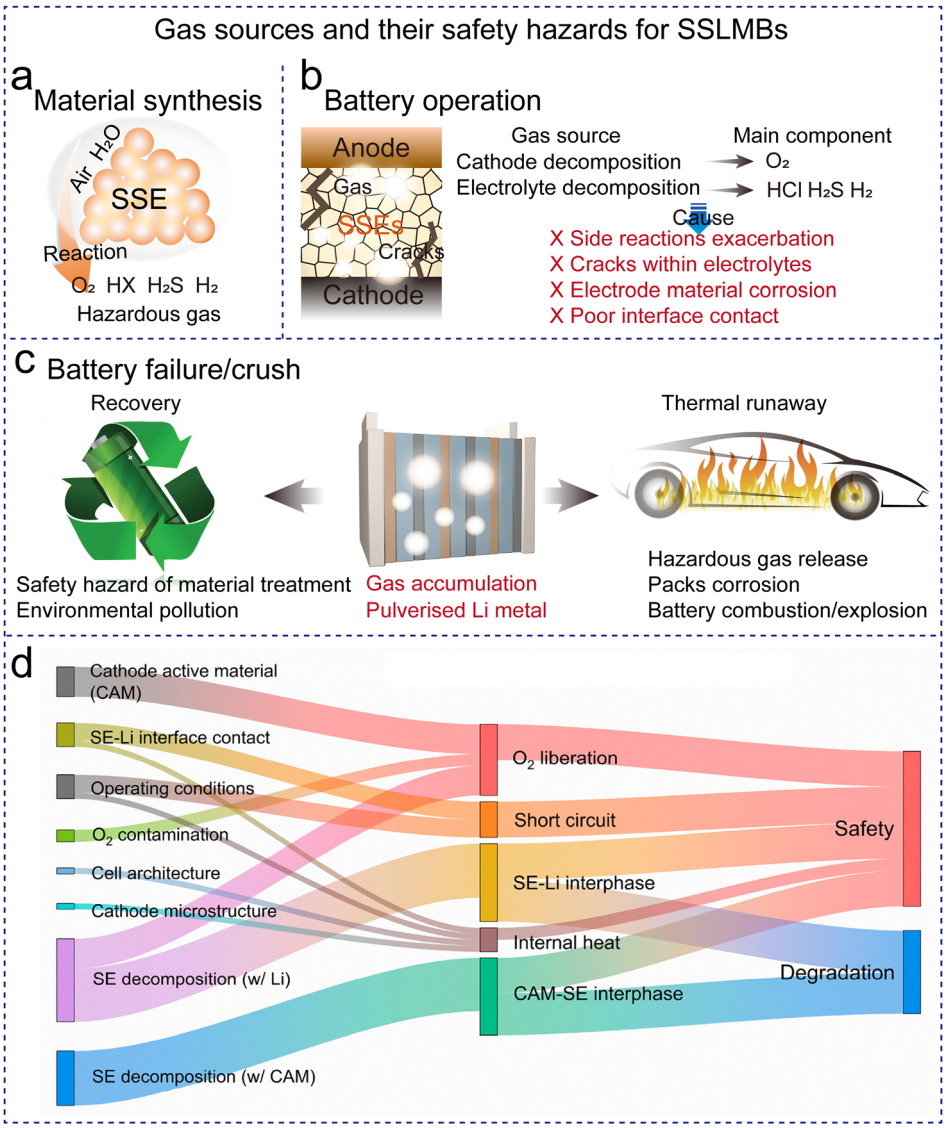

Fig. 4 (a)–(c) Gas sources and corresponding safety hazards for SSLMBs. (d) Safety landscape for SSLMBs. Reproduced with permission from ref. 52.

Moreover, the gases derived from interfacial reactions during battery operation may accelerate side reactions and deteriorate interfacial contact, resulting in interfacial impedance increase and fast battery capacity decay (Fig. 4b). What's worse, the gases (such as O_2) may continuously react with Li or other components and cause significant heat release and internal temperature rise, eventually leading to the thermal runaway of SSLMBs. Notably, battery recycling and post-treatment processes may be accompanied by the release of massive amounts of harmful gases, leading to the destruction and corrosion of battery packs, and even combustion and explosion (Fig. 4c). Furthermore, gas accumulation, pulverized Li metal and unstable SSEs in the spent batteries pose a huge safety hazard to their recycling management.[51] Thus, it is a critical path to enhance the stability of SSLMBs *via* rational design of electrode materials, SSEs, and electrode/SSE interfaces as well as building an appropriate safety management/recycling system.

In brief summary, SSLMBs are not completely safe, as heat accumulation, gas release, and short circuits will cause degradation and thermal runaway of SSLMBs[52] (Fig. 4d). More comprehensive correlative characterization is advised to explore the gas release mechanism and the thermal behavior of SSLMBs, thus, guiding the exploration of targeted improvement strategies.

3. Recent advances in improving the safety of SSLMBs

To address the aforementioned issues, this section focuses on enhancing the safety of SSLMBs by improving the thermal/chemical/electrochemical stability of SSEs and the corresponding interfacial stability of electrode/SSE materials.

3.1. SSE stability improvement

As aforementioned, the air/moisture instability of inorganic solid electrolytes and poor thermal stability of SPEs are critical issues that hinder the development of high-safety SSLMBs. In the following section, we will summarize the recent progress in enhancing the chemical stability of inorganic solid electrolytes and the thermal stability of SPEs.

3.1.1. Inorganic solid electrolyte's structural tuning to enhance chemical stability. As mentioned in Section 2.1.1, inorganic solid electrolytes mainly suffer from severe chemical instability during material preparation. After decades of research, elemental doping and surface coating are two common and effective strategies employed to improve the humidity stability of inorganic solid electrolytes. Taking sulfide SSEs as a typical example, according to the hard soft acid base (HSAB) theory, the PS_4^{3-} group tends to react with H_2O in air to release H_2S gas. Here the substitution of hard acid P^{5+} with soft acids including In^{3+}, Ge^{4+}, Sn^{4+}, As^{5+}, and Sb^{5+} can enhance moisture stability. According to the thermodynamics analysis, the humidity resistance stability of sulfides using these soft acids as the only central cations follows the order of $In^{3+} > As^{5+} > Sn^{4+} > Ge^{4+} > Sb^{5+}$.[20,53] The theoretical analysis is further validated by experiments. For instance, the In-doped $Li_7P_{2.9}S_{10.9}In_{0.1}$ electrolyte exhibited enhanced moisture stability as In partially replaced P, and H_2S release was also significantly decreased.[54] The H_2S released from the $Li_7P_{2.9}S_{10.9}In_{0.1}$ electrolyte was less than 0.25 $cm^3\ g^{-1}$ after being exposed to 20% humid air for 210 s, which is 1/6 of that released from the $Li_7P_3S_{11}$ electrolyte ($\sim$1.50 $cm^3\ g^{-1}$). Similarly, Sb-doping also proved its positive effect in suppressing H_2S release in the Li_6PS_5Cl-based SSEs. It was found that the concentration of H_2S gas released from $Li_6P_{0.925}Sb_{0.075}S_5Cl$ is 0.09 $cm^3\ g^{-1}$, which is much lower than that from Li_6PS_5Cl (0.57 $cm^3\ g^{-1}$) after being exposed to air for 1 h.[55] Moreover, the positive effect of Sb and Sn doping on enhancing moisture stability and suppressing H_2S release was also reported.[56,57] Nevertheless, these phosphorus-based sulfide SSEs still suffer from irreversible structural degradation and H_2S gas release. Therefore, a phosphorus-free sulfide SSE has been developed through complete substitution, which exhibits improved moisture stability and even recoverability after heat treatment. When the P in Li_6PS_5I was substituted by As and Si, the chemical stability was improved, where the H_2S release in Li_6PS_5I was 105.35 $cm^3\ g^{-1}$ after moisture exposure for 20 min (humidity: 23–25%), while the H_2S release in Li_6AsS_5I and $Li_{6.8}Si_{0.8}As_{0.2}S_5I$ (Fig. 5a) was reduced to 75.07 $cm^3\ g^{-1}$ and 91.32 $cm^3\ g^{-1}$. The result can be attributed to the tight bonding between soft acid As^{5+} and soft base S^{2-}.[20]

Besides the sulfide SSEs, the doping strategy has also proved to enhance the humidity stability of halide SSEs.[60] Among the available halide SSEs, Li_3InCl_6 is considered relatively stable in ambient air in the chloride system, and can even be synthesized by water-mediated synthesis.[61] However, recent results suggested that Li_3InCl_6 degraded upon exposure to humid air: Li_3InCl_6 reacts with H_2O to form In_2O_3, LiCl, and corrosive HCl.[25] When Cl was partially replaced by F in Li_3InCl_6 (labeled as $Li_3InCl_{5.6}F_{0.4}$), the water absorption rate was reduced by 3 times from 0.607 g h^{-1} to 0.198 g h^{-1}, while the ionic conductivity decreased from 4.5 times to 1.7 times in the 20 $\pm$ 3 °C dew-point dry room, indicating the improved moisture stability.[62]

The element doping strategy can regulate the inorganic solid electrolyte crystal structure, yet are not useful on the crystal surface where the hydrolysis reaction first occurs. The surface coating or core–shell nanostructure strategy is a valid approach to resist chemical attack by O_2, H_2O and even electrodes for inorganic solid electrolytes. To date, polymers, metal oxides, air-stable inorganic solid electrolytes, and fluorides are commonly used surface layer materials that are expected to inhibit the decomposition and rupture of SSEs (Fig. 5b). For instance, to enhance the moisture stability of Li_3InCl_6, a thin Al_2O_3 coating layer was created by atomic layer deposition (ALD, labeled as $Li_3InCl_6@Al_2O_3$), which reduced the water absorption rate to 1/4 and prolonged the liquefaction time to 7 times compared with the coating-free Li_3InCl_6.[63] In another case, a sulfide SSE with an oxysulfide shell was designed to prevent deterioration of the bulk SSE by moisture.[64] When exposing the SSE to 35% humid air for 5 min, the ionic conductivity of the

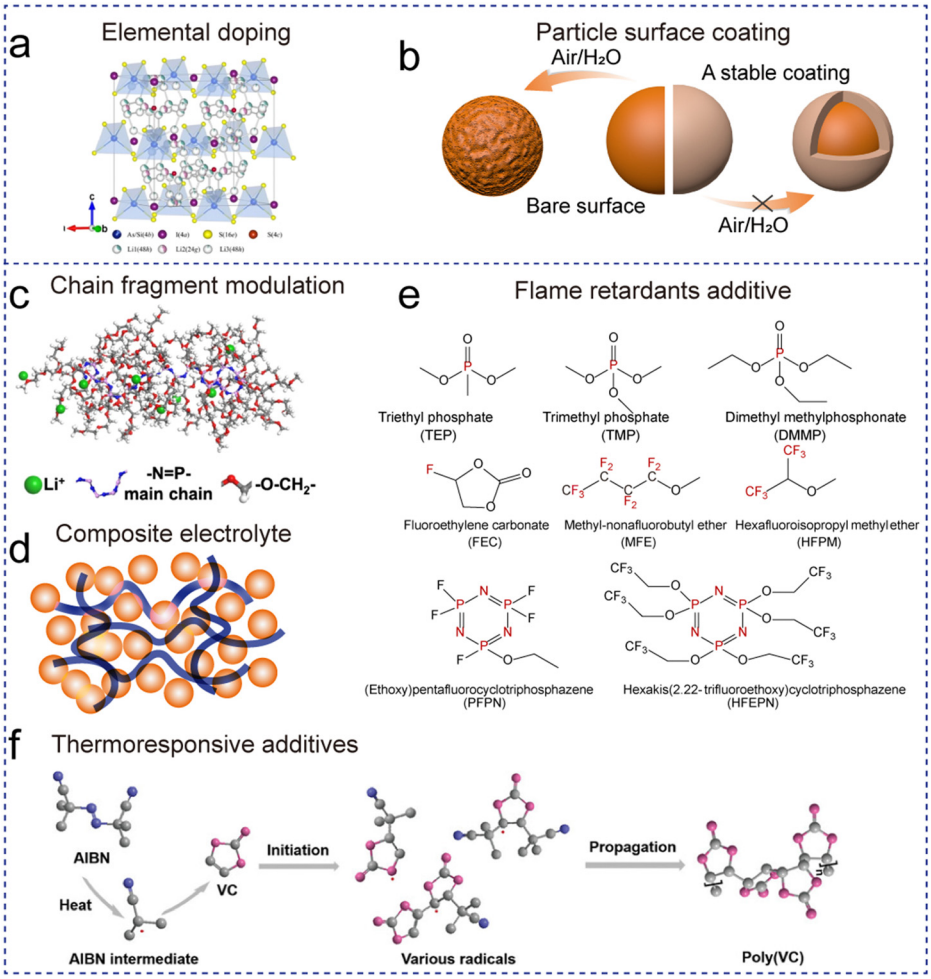

Fig. 5 Electrolyte design strategies. (a) Crystal structures of LASI and LASI-80Si. Reproduced with permission from ref. 20. (b) Inorganic solid electrolyte's surface coating. (c) Liquid-state brush-like polymer PPZ. Reproduced with permission from ref. 58. (d) Inorganic–polymer composite electrolytes. (e) Chemical structures of flame retardants. (f) Schematic illustration of thermal polymerization of VC with AIBN as its initiator. Reproduced with permission from ref. 59.

SSE with the oxysulfide shell slightly decreased by 4.53%, which is only 21% of the coating-free SSE (21.7%).

3.1.2. SPE design to enhance thermal stability

(1) Thermal stability improvement. Polymer matrices typically offer superior chemical stability and air tolerance, whereas their thermal stability is not satisfactory. Actually, the stability of SPEs primarily depends on the chemical structure of the polymer monomer, the degree of crystallinity and other components. Taking PEO as an example, it possesses a relatively low melting point (65 °C). The crystallinity would be reduced and enable the PEO to exhibit a high ionic conductivity of over 10^{-4} S cm^{-1} when the temperature is over 60 °C, while an ultralow room-temperature ionic conductivity of roughly 10^{-8} S cm^{-1} is presented due to the low dissociation degree of Li salt in highly crystalline PEO.[65] However, PEO will thermally decompose and release gas at 330 °C.[66] To enhance the thermal stability of PEO-based SPEs, some thermostable polymers (such as poly(*m*-phenylene isophthalamide) (PMIA), poly(tetra-fluoroethylene) (PTFE), poly(vinylidene fluoride) (PVDF)) are introduced as reinforcement matrices.[16,67,68] In particular, fluorinated polymers possess high T_m (>155 °C) and high T_{dec} (>350 °C) owing to the strong C–F bond, which improves the thermal stability of as-prepared SPEs.[69] A fly in the ointment is that the ionic conductivity of such fluorinated polymer-based SPEs is still unsatisfactory.[70] Polyimide (PI), possessing excellent thermal stability up to 500 °C and chemical inertness, is another promising electrolyte host.[71] Cui's group designed safe SPEs *via* filling PEO/LiTFSI into an 8.6-μm-thick nanoporous polyimide (PI) film to improve the thermal stability of PEO-based SPEs.[72] Then they further introduced decabromodiphenyl ethane (DBDPE) as a flame retardant to improve the safety of SSLMBs.[73] Such a PI/DBDPE SPE ensures stable running of Li|Li symmetric batteries for 300 h without short circuits owing to its thermal stability, non-flammability, and high mechanical strength. More eye-catching evidence of the improved safety is provided by the pouch cells, which work properly even when tested under flame.

Alternatively, dispersing inorganic fillers[74] and fast Li-ion conductors[75,76] into SPEs to integrate composite electrolytes

has been adopted to improve the ionic conductivity, mechanical properties, and thermal stability (Fig. 5d). Firstly, inorganic fillers improve ionic conductivity by inhibiting polymer matrix crystallization and promoting the dissociation of Li salts, as well as providing rich migration sites of Li^+ drawing on their Lewis acid–base groups and oxygen vacancy. Secondly, inorganic fillers possess excellent chemical stability and non-flammability, improving the thermal stability of SPEs. For example, the introduction of 10% $Zn_2(OH)BO_3$ and 30% $Li_{6.4}La_3Zr_{1.4}Ta_{0.6}O_{12}$ (LLZTO) improved the T_{dec} of the PEO SPE from 350 °C to 428–458 °C and 400 °C, respectively.[77,78]

Besides decomposition at high temperatures, PEO-based SPEs will undergo exothermic reactions and may release large amounts of heat/gas during combustion, and introducing flame retardant functional groups is of significance to prevent the thermal runaway in SSLMBs. In this regard, a nonflammable liquid polymer electrolyte (LPE) was designed by using a liquid-state brush-like polymer (consisting of flame-retardant polyphosphazene as the backbone and methoxytriethoxy substituents as the side chains) as the sole solvent (Fig. 5c).[58] Significantly, such a non-flammable LPE enables the full cells to stably run for over 1000 cycles in a wide operating temperature range of 60–90 °C. Besides, the maximum heating rate was only 0.49 °C min^{-1}, and no thermal runaway occurred throughout the accelerating rate calorimeter test.

(2) Flame retardants/thermoresponsive additives. In addition to the polymer structural design, the introduction of flame retardants is another effective strategy to suppress the combustion of SPEs. Generally, flame retardants can be divided into two types: (i) additive-type (*i.e.*, non-reactive inorganic particles or nonflammable polymers) and (ii) reactive-type flame retardants (*e.g.*, phosphate, fluoride and phosphonitrile) (Fig. 5e).[79] The former additives are inert and difficult to react exothermically, thus preventing the combustion of SPEs to a certain extent. In the case of the latter reactive-type flame retardants, their reaction mechanism is as follows: (i) halogen flame retardants firstly produce free radicals $X^\bullet$ (X = F, Cl, Br) after decomposition, and then $X^\bullet$ will capture the highly active free radicals ($H^\bullet$ and $OH^\bullet$) that are produced by the pyrolysis of SPEs. Their decomposition products including HX, H_2O and X_2 dilute the concentrations of combustible gases and O_2, thus delaying the combustion of SPEs. (ii) Phosphorus-based flame retardants will break down and produce phosphate and phosphate oxygen radicals, which diffuse into the gas phase to combine with the combustible radical to delay SPE burning. Meanwhile, phosphoric acid and its derivatives dehydrate the polymer to form a carbon layer that slows down heat transfer and traps O_2, inhibiting the decomposition and combustion of SPEs.[71] For example, triethyl phosphate (TEP) was introduced into an *in situ* polymerized electrolyte to inhibit electrolyte combustion and enhance thermal stability, which enabled the Li metal anode with high temperature (>60 °C) survivability.[80]

Apart from flame retardant additives, thermoresponsive additives have been developed to improve the safety of SSLMBs. The thermoresponsive additives are a class of thermally sensitive materials. They are capable of inhibiting the occurrence of thermal runaway by increasing battery resistance, blocking ion transportation channels, or releasing blocking mediators. Introducing thermoresponsive additives into polymer electrolytes gives LMBs the ability to recognize overheating temperatures in the early stages, which is an effective thermal safety prevention technology. For instance, certain small molecular solvents (vinyl carbonate (VC) and azodiisobutyronitrile) were reported as thermoresponsive electrolytes, which can be polymerized into poly(VC) as the battery temperature abnormally increases (Fig. 5f).[59] The *in situ* formed poly(VC) can act as a barrier to prevent direct contact between electrodes and immobilize the free liquid solvent at high temperatures, thereby reducing the exothermic reactions between electrodes and electrolytes. Consequently, the internal-short-circuit temperature and ''ignition point'' temperature (the starting temperature of thermal runaway) of LMBs are largely increased from 126.3 and 100.3 °C to 176.5 and 203.6 °C, respectively.

3.2. Interface modifications

In Section 3.1, we have summarized the recent advances in developing SSEs with chemical/thermal stability to meet the requirements of safer SSLMBs. Apart from being intrinsically stable, an ideal SSE should be chemically and physically robust with cathodes/anodes, or capable of forming a stable interface as mentioned in Section 2.2, to achieve safer SSLMBs. However, experimental evidence indicates that the safety of SSLMBs is still limited by the undesirable side reactions and dendrite growth due to the mismatched electrode/SSE interface. Furthermore, interfacial exothermic reactions bring about heat accumulation and gas production issues, which tend to cause SSLMBs to heat up and inflate, and more seriously, trigger thermal runaway. In this section, recent advances in terms of electrochemical/thermally stable electrode/electrolyte interlayers and grain boundaries are summarized from an interface engineering perspective to design stable and safe SSLMBs.

3.2.1. Li/SSE interface. Interfacial stabilization strategies, such as anode design, interfacial decoration and SSE innovation have been proven to be effective in inhibiting Li dendrite growth and improving interfacial compatibility between the Li anode and SSEs (Fig. 6a). For instance, designing 3D hosts[81,82] to reduce local current density using uniform Li deposition and developing alloy anodes (Li–Al, Li–In)[83,84] to reduce pure Li reactivity. These approaches help suppress Li dendrite growth to some extent, but the exposed conductive metal surfaces still face the issues of reacting with SSEs. More seriously, the mismatched Li/SSE interface as mentioned in Section 2.2.2 is a tricky concern that needs to be addressed urgently.

Compared with SPEs, the interfacial stability of inorganic solid electrolytes is primarily influenced by the interfacial reaction and interfacial contact resistance. As described in Section 2.2, some SSEs such as NASICON and LGPS may react with the Li metal anode, resulting in electrolyte decomposition and heat emission. Furthermore, a ''point-to-point'' solid–solid contact interface due to rigid inorganic solid electrolytes (especially crystalline oxide SSEs) also leads to large interface resistance,

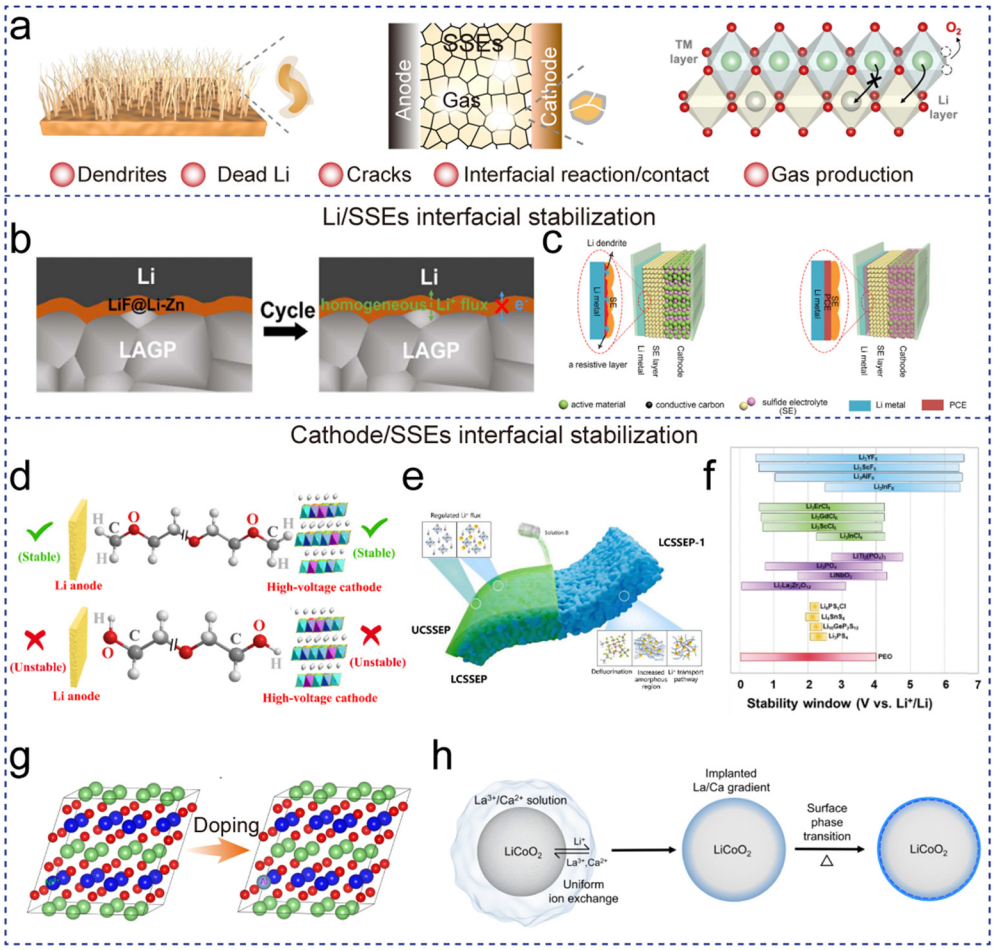

Fig. 6 Interface engineering. (a) Interfacial issues of SSLMBs. (b) Interface evolution between metallic Li anode and ZnF_2 layer-coated LAGP. Reproduced with permission from ref. 85. (c) Schematic diagram of SSLMBs without or with the PCE interlayer. (d) The stability of PEGDME and PEG in contact with the anode and high-voltage cathode. Reproduced with permission from ref. 86. (e) Structure of the Janus composite electrolyte and schematic description of the fabrication of the JCSSE. Reproduced with permission from ref. 87. (f) The electrochemical stability windows of various SSEs. Reproduced with permission from ref. 88. (g) Cathode material crystal structure doping. (h) A protective coating on the $LiCoO_2$ surface based on ion exchange reactions. Reproduced with permission from ref. 89.

uneven current distribution as well as dendrite growth. To solve the issues, functional interlayers such as lithiophilic alloy layers (Ag, In, *etc.*)[90,91] are developed to regulate Li^+ deposition.[92] For instance, a LiF@Li–Zn alloy layer was constructed at the LAGP|Li interface (Z-LAGP) *via in situ* conversion reactions, which exhibited a strong wetting interaction with Li metal and low interfacial resistance, and provided a homogeneous Li-ion flux (Fig. 6b).[85] As a consequence, the Li|Z-LAGP|Li cells presented a critical current density (CCD) of 2.0 mA cm^{-2} and a long lifespan of 1000 h at 0.1 mA cm^{-2}. Notably, although facing similar challenges as alloy anodes, lithiophilic alloy layers help regulate Li-ion flux and suppress Li dendrite growth, but the side reaction still exists due to the mixed conductive layer. Thus, flexible polymer buffer layers (PEO, Kevlar aramid nanofiber)[93,94] have been developed to facilitate intimate interfacial contact. For example, the solid-state plastic crystal electrolyte (PCE) acting as a flexible interlayer can effectively suppress the reduction of Ge^{4+} into metallic Ge, thus inhibiting the decomposition of LGPS at the Li/LGPS interface (Fig. 6c).[95] As a consequence, the assembled Li|S full cells showed stable cycling performance for over 100 cycles at 0.13 mA cm^{-2}.

3.2.2. Cathode/SSE interface. Similar to the Li/SSE interface, the rational design of the cathode/SSE interface is equally important. The cathode/SSE interface suffers from decomposition of the SSE under high voltage (>4 V) and O_2 release from $LiTMO_2$ cathode materials. To address this issue, in this section, advanced strategies will be overviewed from two perspectives: SSE design (*e.g.* bilayer electrolytes, elemental doping, composite electrolytes) and cathode material modification (*e.g.*, crystal structure modulation/doping, surface coating).

(1) High anti-oxidation SSEs. In high-safety SSLMBs, an ideal SSE should possess a wide electrochemical stability window, being stable against both anode and cathode materials. Although PEO-based SPEs have demonstrated high stability against the Li anode, their oxidation potential is below 4.0 V, which can hardly match with the high-voltage cathode materials.[88] On the cathode side, the electrochemical oxidation

of SSEs on the surface of the cathode results in the formation of a passivating layer and subsequently increases interfacial resistance, and even gas release. Based on the simulation and experiments, –OH in the PEO-based SPEs will be oxidized into –COOH(Li), which is the limiting factor of electrochemical stability windows for PEO-based SPEs (Fig. 6d).[86] End-group substitution ($-OCH_3$)[86] or the introduction of inorganic particles (*e.g.*, Al_2O_3, SiO_2)[96,97] interacting with –OH had a positive effect on improving the anti-oxidation of PEO-based SPEs. For example, the PEO-based SPE with mono-dispersed ultrafine SiO_2 delivered a high oxidation stability potential of 5.5 V.[96] Alternatively, creating a high-voltage-resistant interlayer for SPEs towards the cathode has also demonstrated a positive effect on inhibiting SPE decomposition.[98,99] For instance, designing conductive coatings of anionic molecules at the interface enabled the Li|NCM cell with a diglyme electrolyte to work stably at 4.2 V.[98] Although the introduction of fillers and interfacial modification can improve the anti-oxidation performance of PEO-based SPEs to some extent, the intrinsic oxidative stability of PEO requires further enhancement.

Alternatively, designing composite electrolytes with both anti-oxidation and anti-reduction is a promising direction. Janus electrolytes (or bilayer or multi-layer composite SSEs) are regarded as promising candidates to achieve high-stability SSLMBs due to their exceptional compatibility with both cathode and anode. Generally, the SSE facing the cathode possesses high antioxidant properties, while the SSE towards the anode presents high anti-reduction properties. As shown in Fig. 6e, a Janus electrolyte with mortise and tenon joints (JCSSE), composed of a poly(vinylidene fluoride-*co*-hexafluoropropylene) (PVDF-HFP)/$Li_{6.4}La_3Zr_{1.4}Ta_{0.6}O_{12}$ layer toward the cathode and a poly(diallyldimethylammonium) bis(trifluoro-methanesulfonyl)-imide (PDADMATFSI)/UiO-66-SO_3Li layer toward the Li anode, is proposed with broadened electrochemical stability windows.[87] The assembled SSLMBs demonstrated good cycling stability for 100 cycles under a charging cutoff voltage of 4.3 V, as well as superior cycling stability in the wide temperature range of 25–100 °C. In another case, a heterogeneous multilayered solid electrolyte (HMSE) was developed with a reduction tolerant polyethylene glycol diacrylate layer facing the Li anode, while an oxidation-resistant poly(acrylonitrile) (PAN) layer contacts with the cathode. The HMSE possesses a wide electrochemical stability window of 0–5 V, enabling Li|NMC811 SSLMBs stably run for over 175 cycles with a high capacity retention of 94.4% at 0.2C (charging cutoff voltage of 4.3 V).[100]

Compared with SPEs, sulfide SSEs possess higher ionic conductivity, even beyond 10^{-2} S cm^{-1} at room temperature. Nevertheless, the narrow electrochemical stability windows in the range of 1.5–2.5 V are considered to be a major obstacle to matching high-voltage cathodes.[101] It is difficult to broaden the electrochemical stability window of sulfide SSEs *via* elemental doping, where the coating technique[102] and composite electrolytes[103] are adopted as alternative strategies to suppress interfacial reactions in sulfide SSE-based batteries.

Generally speaking, the oxidation potentials of oxide and halide electrolytes are satisfactory compared to sulfide electrolytes as shown in Fig. 6f.[88] For oxide-SSEs, garnet-type LLZO shows a wide electrochemical stability window of 0–6 V, and is regarded as a promising SSE to match the high-voltage cathode materials. However, the large interfacial resistance because of rigid oxide SSEs is a limitation. To solve the issue, the following strategies are adopted: (1) cathode/electrolyte co-sintering to enable the amorphous oxide SSE to crystallize on the surfaces of electrode particles and the electrode materials embedded within the lattice of the oxide SSE, guaranteeing intimate interface contact;[104] (2) introducing high-voltage resistant polymers as a buffer layer; and (3) introducing materials with low melting points (*e.g.* Li_3PO_4) as an intermediate phase to bridge the active materials and SSEs together, ensuring good contact. For instance, the low-melting-point Li_3PO_4 helps build a compatible and Li^+-conductive self-integrated layer to provide continuous Li^+ transport pathways at the NMC811/LLZTO interface. The conclusion is confirmed by the density functional theory (DFT) calculation. The surface energy differences of NCM811/Li_3PO_4 and Li_3PO_4/LLZTO are 0.87 and 0.98 J m^{-2}, which are lower than that of NCM811/LLZTO (1.85 J m^{-2}), indicating the faster Li^+ transport across the NCM811/Li_3PO_4 and Li_3PO_4/LLZTO interfaces. Generally speaking, high-safety and high-voltage SSLMBs are still one of the most interesting routes and more efforts should be devoted to reducing interfacial impedance.[105]

Halide SSEs have recently emerged with relatively high oxidation potentials over 4.2 V (especially for the Cl- and F-based halide SSEs).[60,106] Altering halogen anions could adjust the oxidation stability of halide SSEs ($F^- > Cl^- > Br^- > I^-$); *e.g.*, Li_3YCl_6 shows a wider electrochemical stability window of 0.62–4.21 V than Li_3YBr_6 (0.59–3.15 V).[106] Nevertheless, chloride electrolytes still struggle to satisfy high-voltage demands. Thus, an F-substitution strategy is proposed to achieve the above targets. For instance, 20% Cl in Li_3InCl_6 was substituted with F to obtain the $Li_3InCl_{4.8}F_{1.2}$ SSE, which extended the oxidation stability potential from 4.3 V to over 6 V.[107] DFT was employed to clarify the underlying mechanism, and it was found that an F-containing CEI was formed on the cathode materials, thus suppressing the further decomposition of SSEs under high voltages. It should be mentioned that the SSLMBs using the high voltage LCO cathode still present fast capacity decay, indicating the existence of interfacial side reactions. Thus, developing high-ionic-conductivity fluoride-based SSEs that are compatible with high-voltage cathode materials is highly recommended in the next step.

In brief summary, designing SSEs with high voltage resistance is of significance in achieving high-voltage and high-safety SSLMBs. Considering the intrinsic poor anti-oxidation ability of sulfide SSEs and SPEs, multi-layered SSEs or coating strategies are advised for stabilizing the interface. The rigid oxide and halide SSEs possess high voltage stability, whereas the interfacial contact with cathode materials should be improved.

(2) Cathode oxygen release inhibition. As mentioned in Section 2.2.1, the structural stability of layered oxide $LiTMO_2$ cathodes against O_2 release depends predominantly on their

chemical composition (*e.g.* lithium content and TM species) and SSE/cathode interfacial reaction.[108] Firstly, higher Ni content in $LiTMO_2$ cathodes triggers lower onset temperatures for phase decomposition and more severe oxygen loss attributed to the instability of Ni–O bonding in the charged cathode. Computational results indicate that the TM–O bond strength increases as Ni^{2+}–O < Ni^{3+}–O < Co^{3+}–O < Mn^{4+}–O.[109] Meanwhile, lower Li content (*i.e.*, higher state of charge, SOC) in $LiTMO_2$ cathodes causes structural instability and more O_2 release at elevated temperatures.[110] Secondly, SSE/cathode interfacial reactions will consume surface-activated oxygen and promote bulk-to-surface oxygen migration, aggravating the reaction and releasing massive heat, in turn causing an explosion.[111] Doping with strong covalent elements (Mg, Al, *etc.*)[112,113] has been demonstrated to be an effective approach to thermodynamically stabilize the lattice oxygen (Fig. 6g). The bonding energy is closely related to the covalency of the chemical bond: the more the covalent bonds, the more the delocalized electrons, and the easier for the bond to break. For example, Al and Mg doping has been proven effective in postponing O_2 evolution and reducing heat release as the bonding energy follows the order Al–O/Mg–O > Ni–O > Co–O. To characterize gas evolution from cells, online electrochemical mass spectrometry (OEMS) is employed at high voltages of 4.4 V. The amount of gas released is as follows: $LiNi_{0.90}Mn_{0.05}Al_{0.05}O_2$ (207 μmol m^{-2}) < $LiNi_{0.90}Mn_{0.10}O_2$ (239 μmol m^{-2}) < $LiNi_{0.90}Co_{0.05}Al_{0.05}O_2$ (290 μmol m^{-2}) < $LiNi_{0.90}Mn_{0.05}Co_{0.05}O_2$ (336 μmol m^{-2}) < $LiNi_{0.90}Co_{0.10}O_2$ (513 μmol m^{-2}).[114] The above experimental characterization demonstrates the gas release of cathodes is dependent on the identity of the dopant in the lattice. Apparently, Mn and Al are effective dopants to suppress gas release from overcharged cathodes. Surface coating[89,115–117] is another strategy to hinder interfacial reactions, thus stabilizing the structure of $LiTMO_2$ and against oxygen release. Recently, a Li-poor perovskite structure protection shell and a La/Ca gradient-doped layered-structure buffer layer were constructed to stabilize $LiCoO_2$ (La-LCO) based on ion exchange reactions (Fig. 6h). *In situ* differential electrochemical mass spectrometry (DEMS) was performed to detect gas evolution at first charging. It was found that pristine-LCO exhibits severe O_2 (onset at ~4.33 V) and CO_2 (onset at ~4.17 V) release, while the release is delayed for La-LCO (no O_2 release up to 4.7 V and low content CO_2 emission onset at ~4.57 V). The constructed surface architecture helped suppress surface oxygen and gas release, enabling the assembly pouch cells to stably cycle at 4.8 V.[89] Based on the above results, crystal structure optimization, surface engineering and coating by high-oxygen-activity passivation are promising directions.

3.2.3. Grain boundary decoration. Although interfacial modifications may inhibit side reactions and dendrite growth, inorganic solid electrolytes also face other issues that must be addressed. On one side, dendrites may grow along grain boundaries of inorganic solid electrolytes, resulting in volume expansion and fragmentation of inorganic solid electrolytes. Furthermore, the electronic conductivity may be increased when inorganic solid electrolytes are reduced during cycling, resulting in Li ions nucleating and growing along the interior of inorganic solid electrolytes. Last but not least, internal charge and gas accumulate at grain boundaries and vacancies, accelerating dendrite growth, gas release and crosstalk within SSLMBs. With this in mind, further modification, such as modifying grain boundaries, reducing the electric conductivity and eliminating cracks and defects in SSEs, is urgent to improve the safety of SSLMBs.

(1) Modifying grain boundaries. Introducing ionic-conducting polymers or inorganic compounds at the grain boundaries is promising to alleviate Li dendrite growth. Recently, Yang *et al.* proposed a grain-boundary electronic insulation (GBEI) strategy, aiming to block electron transport *via* introducing an insulating polymer layer (Fig. 7a).[118] Benefitting from the GBEI strategy, Li|Li symmetric cells with 30 times longer lifespan and Li|$LiCoO_2$ full cells with 3 times lower self-discharging rate than pristine sulfide SSEs were developed. Furthermore, $LiPO_2F_2$ was introduced into LATP during ceramic sintering, to suppress the reactions between Li *via* modifying the defect sites inside the LATP pellet (Fig. 7b).[50] Also, the delayed thermal runaway of the LATP pellet with $LiPO_2F_2$ confirmed the as-proposed feasibility of the grain boundary modification strategies.

(2) Reducing electronic conductivity of inorganic solid electrolytes. Notably, the non-negligible electronic conductivity of inorganic solid electrolytes will induce Li deposits inside inorganic solid electrolytes and self-discharge. Recent experimental research showed that this "bulk" dendrite growth is more prevalent in SSEs with high electronic conductivity. To resist dendrite growth, the empirical upper limit thresholds of electronic conductivity should be controlled at 10^{-10} and 10^{-12} S cm^{-1} under current densities of 1 and 10 mA cm^{-2}, respectively.[120] Nevertheless, the electronic conductivity of most reported inorganic solid electrolytes is in the range of 10^{-9} to 10^{-7} S cm^{-1}.[121] To reduce the electronic conductivity, a low-electronic-conductivity sulfide SSE was synthesized by microwave-induced thermal shock to enhance crystallization and suppress carbonization. The obtained microwave-derived Li_6PS_5Cl exhibits an electronic conductivity of 1.2×10^{-9} S cm^{-1}, which is 4 orders of magnitude lower than that of furnace-derived Li_6PS_5Cl (1.7×10^{-5} S cm^{-1}).[122] However, recent research found that the reported electronic conductivity of inorganic solid electrolytes is inconsistent with the large bandgaps (*e.g.*, 5.79 eV for c-LLZO, 3.7 eV for β-Li_3PS_4) computed from DFT.[123] Theoretically, inorganic solid electrolytes should possess an ultralow electronic conductivity of lower than 10^{-10} S cm^{-1}. The huge deviation between experimental and theoretical results is attributed to the cracks and defects that affect electronic transport.[121] Thus, the cracks and defects are suggested to be eliminated to suppress Li dendrite growth.

(3) Eliminating cracks and defects. The formation of cracks and defects in the SSE during the Li plating process is another reason leading to the short circuit and thermal runaway.

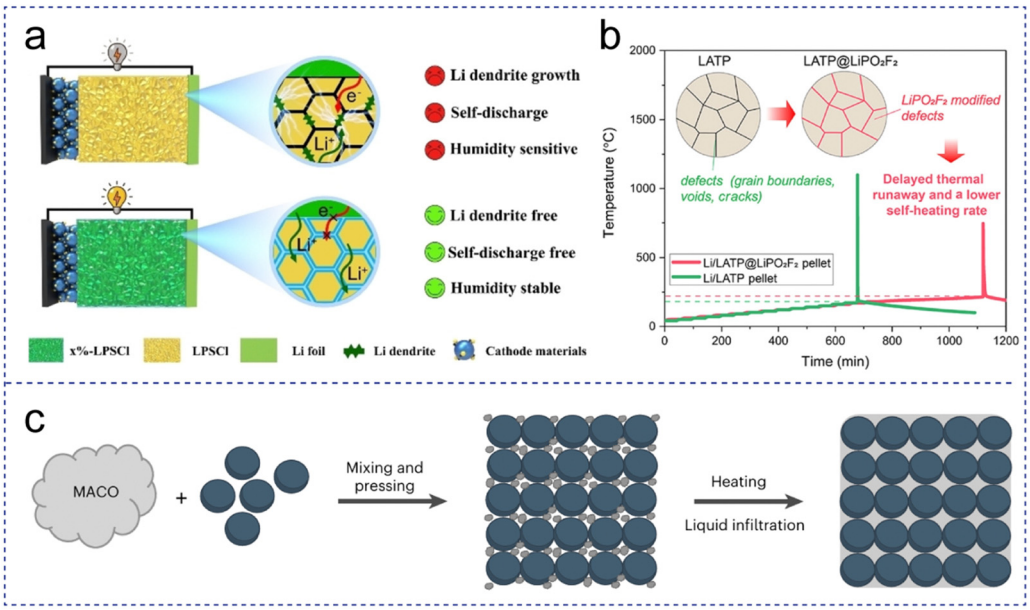

Fig. 7 Grain boundary decoration. (a) Schematic illustrations of SSLMBs with and without PEGDME modified LPSCl electrolytes. Reproduced with permission from ref. 118. (b) ARC test results of the Li/LATP pellet and the Li/LATP@LPF-pellet sample. Reproduced with permission from ref. 50. (c) A schematic diagram of the VIGLAS-based electrode fabrication process. Reproduced with permission from ref. 119.

To reduce the cracks and defects that arise in the SSEs, designing an integrated electrolyte structure[124] or increasing operating pressure[125] can be considered. Apparently, external stack pressure helps reduce the porosity of the SSE pallet and interfacial impedance.[126,127] Nevertheless, higher stack pressure may short-circuit the cell during battery preparation immediately or after a few cycles. This stems from the inherent ductility of the Li metal, allowing Li to creep through the pores of the SSEs. Hence, an appropriate stack pressure should be adopted to enable the stable cycling of SSLMBs.[128,129] Alternatively, compared with crystalline SSEs, amorphous SSEs present the primary advantages of softness, easy fabrication, low grain boundaries, wider compositional variations, and isotropic ionic conductivity.[83,119,130] Recently, a viscoelastic inorganic glass (VIGLAS) was reported to serve as a SSE by simply replacing the chlorine of tetrachloroaluminates with oxygen.[119] The VIGLAS with polymer-like mechanical properties holds great promise, which improves the mechanical stability of inorganic solid electrolytes and enables the successful operation of pressure-less SSLMBs (<0.1 MPa, Fig. 7c).

3.3. Advanced analytical technique

Previously, we summarized failure mechanisms of SSLMBs and strategies for manipulating SSEs and electrode/SSE interfaces to enhance their safety. This section focuses on advanced characterization techniques and theoretical analysis for mechanistic studies of SSLMBs, including heat evolution, dendrite growth, gas emission, *etc.* (Fig. 8).

(1) Heat evolution. Differential scanning calorimetry (DSC) and accelerating rate calorimetry (ARC) are two common techniques for thermal analysis. The former mainly offers information on the heat generation of each battery component by evaluating the enthalpy (ΔH) value.[134] The latter has the merits of the former, meanwhile evaluating the thermal hazard of the whole battery.[135] Employing the ARC, some of the critical kinetic parameters, *i.e.* the onset temperature of the reaction and the enthalpy of the exothermic process, can be acquired. For example, ARC was employed to analyze the sulfide SSE/Li interfacial reaction. The results showed that the $Li_{10}SnP_2S_{12}$ (LSPS)/Li interface exhibited an exacerbated thermal runaway compared with the Li_6PS_5Cl/Li and Li_3PS_4/Li interfaces. Furthermore, ARC was also used to evaluate the thermal safety of LIBs (with graphite anode) and SSLMBs. The results showed that SSLMBs required a larger temperature for thermal runaway onset (295.0 °C for the uncycled LSPS-based cell, *vs.* 90 °C for the LIB). Accompanied by rapid self-exothermic reaction, LSPS-based batteries achieve maximum temperatures of 412.7 °C. Moreover, attributed to the highly exothermic reaction of the Li metal anode with both the SSE decomposition products and O_2 releasing from the cathode, it was inferred that the total heat generated in the SSLMBs is over 3 times that of LIBs.[52]

(2) Battery gas production. Gas production is a challenging issue that leads to battery expansion, deformation and thermal runaway, as discussed in Section 2.3. Differential electrochemical mass spectrometry (DEMS) is a valid technique for studying gas release. Based on DEMS, the gas release behavior of the $LiCoO_2$|PEO–LiTFSI|Li cell was explored, and it was confirmed that the $LiCoO_2$ cathode material would catalyze PEO-based SSEs' decomposition at 4.2 V and release H_2 gas.[38] Coating a LATP layer on $LiCoO_2$ could suppress the catalytic effect and thus improve the stable working voltage over 4.5 V. Gas chromatography-mass spectrometry (GC-MS) is another critical technique to quantitatively analyze the gas composition and content. The composition of gases can be used to study and

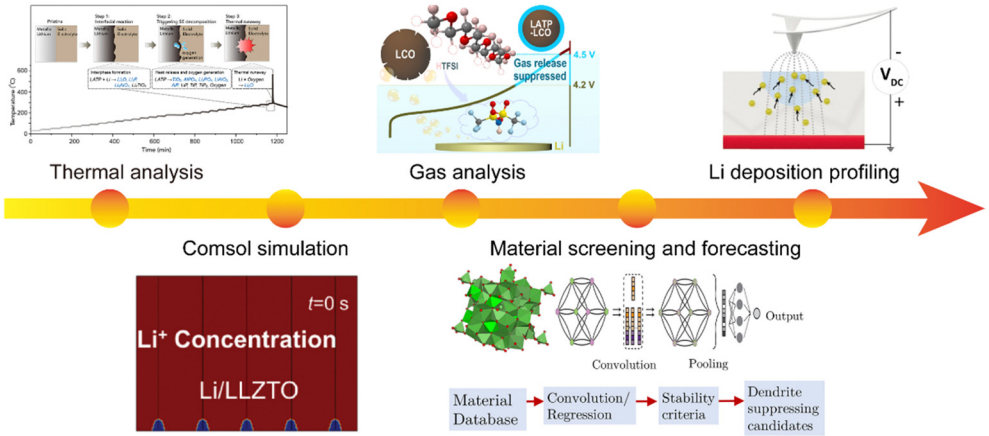

Fig. 8 Advanced analytical techniques to reveal the internal reaction mechanisms of SSLMBs. Reproduced with permission from ref. 14, 38 and 131–133.

reveal the thermal runaway mechanism, and then propose the corresponding solutions.

(3) **Battery short circuit.** Dendrite formation is one of the crucial causes for SSLMB short circuits, while Li deposition behavior and the evolution process are difficult to predict. To date, visible and real-time techniques, including optical microscopy, X-ray tomography (XRT), neutron depth profiling, *etc.*, are intensely developed. For instance, Zhu *et al.* mapped locally time-dependent electric potential changes in garnet-type SSEs, to understand the role of grain boundaries in Li nucleation and dendrite growth *via operando* Kelvin probe force microscopy measurements.[131] A decrease in potential at grain boundaries near the Li anode is observed, resulting in preferential electron accumulation and Li dendrites at grain boundaries. In SSLMBs, soft circuit is also a common phenomenon although rarely noticed due to the lack of simple and effective identification methods. For example, cyclic voltammetry (CV) was proposed to identify and quantify the soft breakdown in Li symmetric SSLMBs.[136] Moreover, low-frequency electrochemical impedance spectroscopy (EIS) was combined to quantitatively analyze the self-discharge of SSLMBs caused by soft breakdown. Furthermore, *operando* neutron imaging and X-ray computed tomography (XCT) were employed to nondestructively visualize Li deposition behaviors and reveal the origins of both "soft" and "hard" shorts in SSLMBs.[137]

In brief summary, the advanced characterization techniques are helpful to comprehensively understand the underlying mechanisms from different angles, and the non-destructive and *in situ* characterization techniques are powerful tools to understand the actual situation and internal evolution of SSLMBs during cycling.

Besides the advanced characterization, theoretical analysis is another powerful strategy to understand the mechanism at an atomic level. COMSOL has been developed to simulate the internal evolution, Li deposition behavior, thermal management and thermal runaway of SSLMBs. For instance, COMSOL multi-physics field simulation was adopted to build a 3D electrochemical model with the coupling of electric and temperature fields, which helps understand the temperature changes[133] and Li dendrite growth.[138,139] Additionally, machine learning (ML) has been widely used to predict properties and learn the rules underlying datasets, thus efficiently simplifying the material-discovery process and performance predictions. Recently, Ahmad and his coworkers screened over 12 000 inorganic materials based on their mechanical properties, aiming to predict their ability to inhibit Li dendrite formation and stabilize the interface as SSEs.[132] Based on ML, they predicted over 20 mechanically anisotropic interfaces with the Li metal anode, and four of them enable dendrite growth suppression. Besides, the screened candidates (*e.g.*, LiOH and Li_2WS_4) are generally soft and highly anisotropic, which show great potential to be high-ionic-conductivity SSEs with strong Li dendrite suppression capability. Although great progress has been achieved, the application of ML still faces two critical challenges: massive data and reliable models. Apparently, the acquisition and screening of reliable data is a priority for the future. More approaches should be explored for material discovery to address the data scarcity challenge. Apparently, advanced analysis techniques reveal the dynamic deposition behavior of the Li anode, as well as the reaction mechanism, gas release and thermal conduction at the interface, which provide a guideline to optimize electrodes, SSEs and their interfaces. In future, the combination of more experimental and computational techniques is suggested to enable deep understanding of the underlying mechanism buried in SSLMBs, guiding the development of safer SSLMBs.

4. Engineering SSLMB design

Apart from developing inert and thermally stable SSEs as well as stabilizing the interface, the operation and post-failure state of SSLMBs need to be considered. In this section, the factors affecting the safety of SSLMBs under practical application and post-processing are discussed to guide and design safer SSLMBs.

4.1. Battery safety management system

As aforementioned, the factors including the material and SSLMB assembly process, the working environment and operating conditions, *etc.*, affect the lifespan and safety of SSLMBs. Besides,

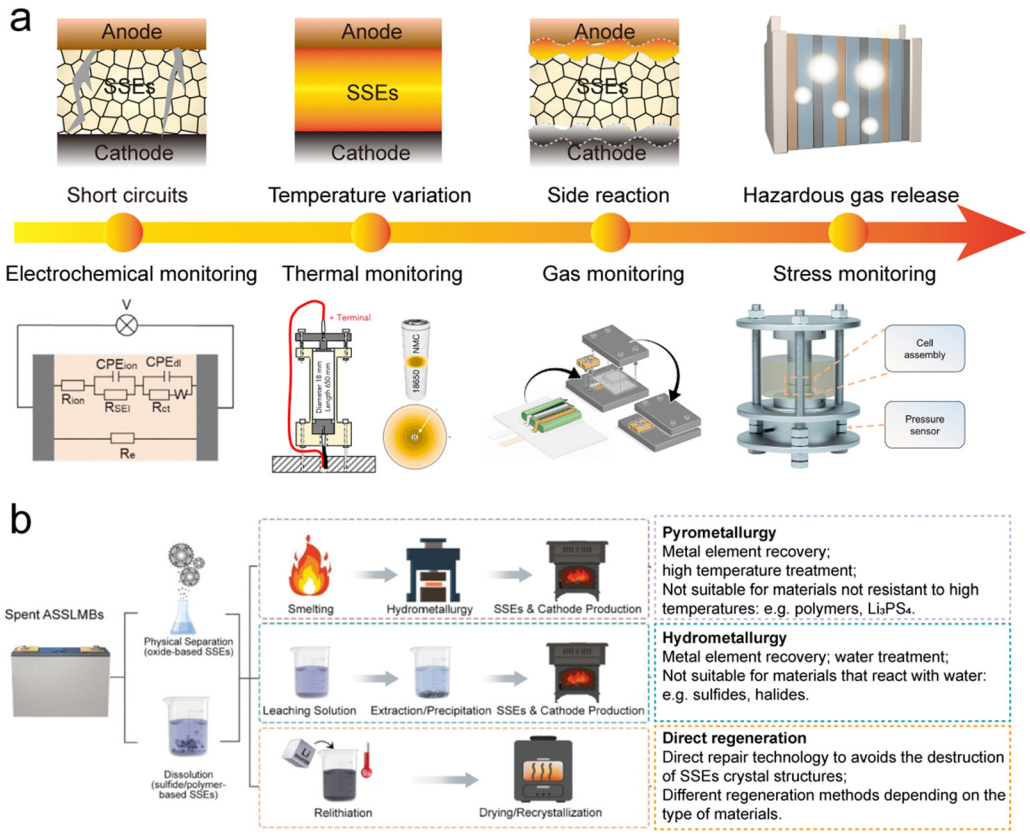

Fig. 9 (a) Potential safety hazards and corresponding monitoring means for SSLMBs. Reproduced with permission from ref. 136 and 141–143. (b) Overview of feasibility and challenges of different recycling technologies for SSLMBs. Reproduced with permission from ref. 144.

given the unpredictable operation environment for grid energy storage and EVs, more reliable state monitoring and safety management of SSLMBs is also required to maintain the optimal working temperature (typically between 25 and 40 °C) and against thermal runaway.[140] Fig. 9a shows potential safety hazards and corresponding monitoring means for SSLMBs. Among the numerous monitoring techniques, electrochemical testing has been widely adopted. Voltage and current are the most important parameters to initially judge whether the SSLMBs work properly. However, it is difficult to diagnose the internal state and predict sudden thermal runaway inside the SSLMBs.

Alternatively, temperature and gas are important signals reflecting thermal runaway, since the internal reactions of SSLMBs are usually accompanied by temperature change and gas release. In the following sections, advanced safety management systems will be discussed according to the above two parameters.

(1) Temperature monitoring and regulation. Early thermal runaway detection methods primarily rely on monitoring the temperature of SSLMBs to prevent them from reaching the onset of thermal runaway. To date, temperature-indication methods including temperature sensors (thermistors, resistance temperature detectors, thermocouples, *etc.*)[145] and thermal imaging technologies (infrared thermography, liquid crystal thermography, *etc.*)[146] are adopted to reflect the temperature changes during battery operation.[147] However, the responsiveness of these early detection systems is limited by the surface-mounted temperature sensors as they cannot precisely reflect the internal state of batteries. Thus, advanced detection systems should be developed to reflect internal temperature changes. Recently, X-ray diffraction (XRD) was utilized to monitor the expansion and/or contraction of the Cu current collector crystal structures of commercial cylindrical cells, achieving real-time and non-destructive internal temperature measurements.[141] First, XRD-computed tomography (CT) was used to obtain full cross-sectional temperature maps, exploring spatial distributions at the end of charge or discharge. Second, a multi-channel collimator (MCC) was used to resolve the temperature within arbitrarily selected internal locations for real-time quantification. The novel non-destructive methodology provides internal temperature evolution information, allowing better monitoring of battery operating conditions.

Detecting the internal temperature changes in SSLMBs not only predicts thermal runaway, but ensures that battery packs work in a safe and mild temperature range by regulating temperature.[148] According to the transferring medium, three thermal management approaches including air cooling, liquid cooling and phase change material (PCM) cooling have been widely used to regulate temperature.[149,150] Notably, the former two approaches generally require additional cooling equipment, decreasing the energy density of the battery systems. Alternatively, PCMs, *via* absorbing/releasing latent heat at the phase change temperature to achieve thermal management,

have attracted much attention due to the non-requirement of auxiliary cooling equipment. Nevertheless, PCMs such as paraffin are limited by low thermal conductivity and flammability. More efforts are recommended to explore non-flammable PCMs with higher thermal conductivity.[151]

(2) Gas analysis and processing. Apart from temperature detection, the gas signals, especially volatile flammable gas derived from SSEs, are another key indicators for predicting SSLMB failure. Gas sensors are very useful in the early detection of thermal runaway in SSLMBs.[142] As mentioned in Section 2, the gas components are highly determined by SSEs and different gases would be released in different SSLMB systems, which put forward higher requirements on the design of characteristic gas sensors. Moreover, the volume expansion and increased pressure would be also accompanied by the gas release. Thus, a pressure sensor is another promising detection means. Accurate measurement of internal stress changes during battery operation is of significance to understand the electrochemical–mechanical effects, thus allowing for a timely early warning of thermal runaway.[143,152] Recently, a compact and multifunctional optical fiber sensor (12 mm in length and 125 μm in diameter) was inserted into commercial 18 650 cells to *operando* monitor internal pressure and temperature during cycling.[153] The two internal pressure peaks of sensor's signal correspond to safety venting and the onset of thermal runaway. The sensor provides a scalable solution to determine the safe warning range of thermal runaway based on the change of the temperature and pressure differential curves. By raising an alert before safe venting, the sensor provides critical abilities for battery safety assessment and thermal runaway warning.

It is worth noting that most gases accumulated in the SSLMBs are toxic, flammable and corrosive, posing a great safety hazard.[154] When thermal runaway occurs, these gases and internal dust particles will be ejected, which will be harmful to human health or even lead to spontaneous explosions. Therefore, it is essential to develop appropriate fire-extinguishing technology. Referring to the experience of LIBs, the current fire extinguishing agents are mainly divided into water-based fire extinguishing agents, air-based fire extinguishing agents, dry powder fire extinguishing agents and aerosol fire extinguishing agents.[155] Here these agents were compared, and water-based fire-extinguishing agents showed the best performance since they possess high cooling capacity and excellent anti-reflash performance for the fire.[156] However, they are not applicable to SSLMBs due to the high activity of Li metal and the low humidity tolerance of SSEs. With this in mind, more efforts should be devoted to developing environmentally friendly and efficient fire extinguishing agents, aiming to build the last safety barrier for SSLMBs when thermal runaway occurs.

4.2. Battery post-processing

Rapid growth in the market for EVs presents post-treatment/recycling challenge for the spent SSLMBs: the safety of spent SSLMBs and recycling of valuable secondary key materials. Here the potential approaches for SSLMB post-treatment/recycling are summarized and future directions are highlighted.

(1) Exhaust gas reprocessing. The safety issues exist not only in the material preparation and SSLMB operation process but also in the treatment of spent SSLMBs. The effect of the gas venting behavior and thermal runaway hazard severity of LFP batteries using three types of safety valves was evaluated and the main conclusion can be seen as follows: (I) LFP batteries with a round safety valve exhibit a maximum gas venting pressure of 3320 Pa, which is one order of magnitude higher than that of the oval or cavity safety valves; (II) the LFP battery using an oval safety valve presented the lowest thermal runaway hazard according to the gray-fuzzy analytic hierarchy process. With this in mind, the gas venting and thermal safety should be considered balanced during the safety valve design.[157] In addition, the treatment of exhaust gases in SSLMBs can refer to LIBs, where the acidic gases (*e.g.* HF, H_2S, *etc.*) can be absorbed by alkaline solutions, while the combustion strategy can be applied to remove H_2.

(2) Spent Li treatment/recycling. SSLMBs possess different types of SSE chemistries and Li metal anodes, which put forward higher requirements on the recycling process. Considering that both the Li anode and SSEs are sensitive to moisture, the dismantling of the spent SSLMBs should be carried out in a low-humidity atmosphere to realize key material recycling.[158] To safely recycle Li, solvents such as ethanol, naphthalene, and diethyl carbonate (DEC) are recommended to dissolve or consume Li metal mildly.[159,160] For instance, Li metal can slowly react with DEC to form Li-DEC, which can be utilized as the raw source to produce Li salts such as Li_2CO_3, LiOH, *etc.*[160] Besides the selection of suitable solvents, the vessel should be also considered. Notably, pulverized Li owing to its lower density tends to float and scatter in the process of separation as an ignition source to cause environmental fires. What's worse, the combustible gas and strongly basic LiOH derived from the reaction of Li metal also put forward higher requirements for the reaction vessel.[161] In other words, to realize the safe Li recycling process, the solvent and vessel should be carefully selected, and the consumption rate and environment should be controlled as well.

(3) SSE recycling. As for the Li anode, special processes or environments are required to recycle the SSEs, especially for the moisture-sensitive sulfide SSEs, where the toxic H_2S gas release is harmful to human health. Fortunately, the successful LIB recycling industry would provide a guideline for future SSLMB recycling. To date, considerable research and reviews have been devoted to developing high-efficiency recycling methods for spent LIBs, and the methods can be generally categorized as pyrometallurgical recycling, hydrometallurgical recycling and direct regeneration.[162–164]

Fig. 9b summarizes and compares the feasibility and challenges of the three recycling technologies. Pyrometallurgy and hydrometallurgy primarily involve the destruction of the crystal structure of the materials at the atomic level and the extraction of valuable metallic elements, while they may be not suitable for all SSEs. Firstly, the pyrometallurgical technique is operated under high temperatures, which accelerates the reaction between gases and dead Li, leading to intense exothermic phenomena. Besides, SPEs and sulfide SSEs would be burned off and could not

be recovered using this method. Different from pyrometallurgy, hydrometallurgy is an aqueous chemical treatment but has certain limitations. For example, Li metal can react violently with water and generate flammable H_2 if not pretreated beforehand. In addition, sulfide SSEs cannot be dispersed in water due to their instability and production of toxic H_2S gas.[144,165] Therefore, it is still urgently required to explore alternative recycling strategies to improve the recycling safety of SSEs. Of the three recycling technologies, direct regeneration is superior in terms of maximizing the economic value and minimizing environmental impact. For instance, polar solvents such as ethanol and acetonitrile are used to dissolve the PS_4^{3-} thiophosphate unit-containing sulfide SSEs, where the sulfide SSEs can be regenerated through heat treatment and relithiation without structural damage and safety hazard.[166,167] However, the recycling of SSEs is still at its infancy, where opportunities and challenges coexist. To accelerate the development of SSLMB recycling technologies, both recycling efficiency and economic benefits should be taken into consideration.

5. Perspectives and outlooks

At present, SSLMBs have proven the most promising next-generation rechargeable batteries for portable electronic devices and stationary energy storage systems in terms of their improved energy density and safety. Nevertheless, challenges such as undesirable safety and lifespan should be addressed to accelerate their path to commercialization.

(1) Advanced SSE development and interface engineering

To the best of our knowledge, heat accumulation and gas production mainly caused by SSE decomposition and interfacial reactions seriously affect the safety of SSLMBs. On one side, more efforts are recommended to be devoted to developing SSEs with high thermal stability, moisture-stability and wide electrochemical stability windows. For example, composite SSEs have demonstrated their merits in extending the electrochemical stability windows and improving the thermal stability while their preparation process and cost need further improvement and refinement.[168] It is proposed to construct multilayer composite SSEs to enhance the antioxidant to cathode side and the anti-reduction to anode side, thus enhancing the overall stabilization of SSEs.[169] Moreover, high-ionic-conductivity fluoride-based SSEs with wide electrochemical stability windows and high thermal stability are also highly recommended. Apart from SSEs, future works would focus on interfacial engineering, *e.g.* constructing flexible insulation layers at the interfaces and grain boundaries. It is recommended to design an ideal interphase with high ionic conductivity and low electronic conductivity, as well as good densification to inhibit interfacial side reactions, thus improving the safety of SSLMBs.[170]

(2) High-throughput screening and advanced theoretical calculations/characterization

Theoretical chemistry facilitates rapid screening of materials and significantly enhances synthesis efficiency. Li's group discovered 12 promising super Li-ion conductors from 29 008 garnets for SSEs using artificial intelligence (AI) technologies. This approach directly cuts across at least 95 years of computational cycles to screen SSEs, accelerating the innovation of SSEs.[171] Advanced theoretical calculation has a huge influence in terms of structural properties, ion transport mechanisms, and material optimization, thus guiding the design of safer materials and SSLMB systems.[172,173] Meanwhile, more *in situ* and coupling techniques are suggested, and theoretical predictions are used to provide more comprehensive evidence. Photoacoustic microscopy techniques[174,175] combining the merits of non-destructive testing, high temporal resolution and three-dimensional imaging are powerful tools to analyze the material structure and the physical properties (*e.g.*, temperature).

(3) Application

To realize the commercialization of SSLMBs, energy density, safety and cycling performance should be balanced. Compared with the high reactivity of Li metal, high-capacity alloying anodes are also a good choice by balancing energy density and safety. To reduce the generation of gas, the internal water content of SSLMBs should be minimized during material preparation and SSLMB assembly. Furthermore, AI-management systems are proposed for real-time battery health monitoring and aging state control, as well as for early warning of abnormal battery operation.[176,177] In addition, advanced sensing technologies are advised during battery operation to obtain valuable data signals. Relying on the collected data, AI-management helps improve the health, efficiency and safety of SSLMBs. Notably, most research has focused on thermal runaway prevention and battery management systems, paying little attention to fire suppression after cell thermal runaway. Delayed combustion systems are suggested in conjunction with early warning systems and fire suppression under extreme conditions (*e.g.* nail penetrations or high temperatures) to promise high safety.[178]

Data availability

This is a review paper. Most of the figures and results used in this review are collected from the publications listed in the references. The remaining data are available upon request.

Conflicts of interest

There are no conflicts to declare.

Acknowledgements

This work is supported by the National Natural Science Foundation of China (No. 22279135, U1808209), CAS Project of Young Scientists in Basic Research (No. YSBR-058), CAS Strategic Leading Science & Technology Program (A) (XDA21070100), CAS Engineering Laboratory for Electrochemical Energy Storage (KFJ-PTXM-027), Natural Sciences and Engineering Research Council of Canada (NSERC), Canada Research Chair Program

(CRC), Canada Foundation for Innovation (CFI), Hebei Natural Science Foundation (B2023202027), and Science and Technology Project of Hebei Education Department (No. JZX2024003, QN2024080).

References

1 J. Xiao, F. Shi, T. Glossmann, C. Burnett and Z. Liu, *Nat. Energy*, 2023, **8**, 329–339.
2 J. T. Frith, M. J. Lacey and U. Ulissi, *Nat. Commun.*, 2023, **14**, 420.
3 Q. Li, C. Geng, L. Wang, Q.-H. Yang and W. Lv, *Renewables*, 2023, **1**, 374–396.
4 A. Yang, C. Yang, K. Xie, S. Xin, Z. Xiong, K. Li, Y.-G. Guo and Y. You, *ACS Energy Lett.*, 2023, **8**, 836–843.
5 S. Kim, G. Park, S. J. Lee, S. Seo, K. Ryu, C. H. Kim and J. W. Choi, *Adv. Mater.*, 2023, **35**, 2206625.
6 Y.-C. Yin, J.-T. Yang, J.-D. Luo, G.-X. Lu, Z. Huang, J.-P. Wang, P. Li, F. Li, Y.-C. Wu, T. Tian, Y.-F. Meng, H.-S. Mo, Y.-H. Song, J.-N. Yang, L.-Z. Feng, T. Ma, W. Wen, K. Gong, L.-J. Wang, H.-X. Ju, Y. Xiao, Z. Li, X. Tao and H.-B. Yao, *Nature*, 2023, **616**, 77–83.
7 S. Zhou, M. Li, P. Wang, L. Cheng, L. Chen, Y. Huang, S. Yu, F. Mo and J. Wei, *Electrochem. Energy Rev.*, 2023, **6**, 34.
8 Y. Li, S. Song, H. Kim, K. Nomoto, H. Kim, X. Sun, S. Hori, K. Suzuki, N. Matsui, M. Hirayama, T. Mizoguchi, T. Saito, T. Kamiyama and R. Kanno, *Science*, 2023, **381**, 50–53.
9 N. Kamaya, K. Homma, Y. Yamakawa, M. Hirayama, R. Kanno, M. Yonemura, T. Kamiyama, Y. Kato, S. Hama, K. Kawamoto and A. Mitsui, *Nat. Mater.*, 2011, **10**, 682–686.
10 Y. Kato, S. Hori, T. Saito, K. Suzuki, M. Hirayama, A. Mitsui, M. Yonemura, H. Iba and R. Kanno, *Nat. Energy*, 2016, **1**, 16030.
11 Y. Tanaka, K. Ueno, K. Mizuno, K. Takeuchi, T. Asano and A. Sakai, *Angew. Chem., Int. Ed.*, 2023, **62**, e202217581.
12 L. Ye and X. Li, *Nature*, 2021, **593**, 218–222.
13 W. Yan, Z. Mu, Z. Wang, Y. Huang, D. Wu, P. Lu, J. Lu, J. Xu, Y. Wu, T. Ma, M. Yang, X. Zhu, Y. Xia, S. Shi, L. Chen, H. Li and F. Wu, *Nat. Energy*, 2023, **8**, 800–813.
14 R. Chen, A. M. Nolan, J. Lu, J. Wang, X. Yu, Y. Mo, L. Chen, X. Huang and H. Li, *Joule*, 2020, **4**, 812–821.
15 L. Han, Y. Liu, C. Liao, Y. Zhao, Y. Cao, Y. Kan, J. Zhu and Y. Hu, *Nano Energy*, 2023, **112**, 108448.
16 S. Yang, X. He, T. Hu, Y. He, S. Lv, Z. Ji, Z. Zhu, X. Fu, W. Yang and Y. Wang, *Adv. Funct. Mater.*, 2023, **33**, 2304727.
17 X. Rui, D. Ren, X. Liu, X. Wang, K. Wang, Y. Lu, L. Li, P. Wang, G. Zhu, Y. Mao, X. Feng, L. Lu, H. Wang and M. Ouyang, *Energy Environ. Sci.*, 2023, **16**, 3552–3563.
18 S. Wang, Y. Wu, T. Ma, L. Chen, H. Li and F. Wu, *ACS Nano*, 2022, **16**, 16158–16176.
19 Z. Gao, H. Sun, L. Fu, F. Ye, Y. Zhang, W. Luo and Y. Huang, *Adv. Mater.*, 2018, **30**, 1705702.
20 P. Lu, Y. Xia, G. Sun, D. Wu, S. Wu, W. Yan, X. Zhu, J. Lu, Q. Niu, S. Shi, Z. Sha, L. Chen, H. Li and F. Wu, *Nat. Commun.*, 2023, **14**, 4077.
21 X. Yang, X. Gao, M. Jiang, J. Luo, J. Yan, J. Fu, H. Duan, S. Zhao, Y. Tang, R. Yang, R. Li, J. Wang, H. Huang, C. Veer Singh and X. Sun, *Angew. Chem., Int. Ed.*, 2023, **135**, e202215680.
22 R. Koerver, I. Aygün, T. Leichtweiß, C. Dietrich, W. Zhang, J. O. Binder, P. Hartmann, W. G. Zeier and J. Janek, *Chem. Mater.*, 2017, **29**, 5574–5582.
23 J. P. Goudon, F. Bernard, J. Renouard and P. Yvart, *Int. J. Hydrogen Energy*, 2010, **35**, 11071–11076.
24 S. Wang, X. Xu, C. Cui, C. Zeng, J. Liang, J. Fu, R. Zhang, T. Zhai and H. Li, *Adv. Funct. Mater.*, 2022, **32**, 2108805.
25 W. Li, J. Liang, M. Li, K. R. Adair, X. Li, Y. Hu, Q. Xiao, R. Feng, R. Li, L. Zhang, S. Lu, H. Huang, S. Zhao, T.-K. Sham and X. Sun, *Chem. Mater.*, 2020, **32**, 7019–7027.
26 W. Li, M. Li, P.-H. Chien, S. Wang, C. Yu, G. King, Y. Hu, Q. Xiao, M. Shakouri, R. Feng, B. Fu, H. Abdolvand, A. Fraser, R. Li, Y. Huang, J. Liu, Y. Mo, T.-K. Sham and X. Sun, *Sci. Adv.*, 2023, **9**, eadh4626.
27 F. Takeiri, A. Watanabe, K. Okamoto, D. Bresser, S. Lyonnard, B. Frick, A. Ali, Y. Imai, M. Nishikawa, M. Yonemura, T. Saito, K. Ikeda, T. Otomo, T. Kamiyama, R. Kanno and G. Kobayashi, *Nat. Mater.*, 2022, **21**, 325–330.
28 Y. Wu, S. Wang, H. Li, L. Chen and F. Wu, *InfoMat*, 2021, **3**, 827–853.
29 C.-W. Wu, X. Ren, W.-X. Zhou, G. Xie and G. Zhang, *APL Mater.*, 2022, **10**, 040902.
30 Z. Gao, S. Rao, T. Zhang, F. Gao, Y. Xiao, L. Shali, X. Wang, Y. Zheng, Y. Chen, Y. Zong, W. Li and Y. Chen, *Adv. Sci.*, 2022, **9**, e2103796.
31 G. Abels, I. Bardenhagen, J. Schwenzel and F. Langer, *J. Electrochem. Soc.*, 2022, **169**, 020560.
32 X. L. Yao, S. Xie, C. H. Chen, Q. S. Wang, J. H. Sun, Y. L. Li and S. X. Lu, *J. Power Sources*, 2005, **144**, 170–175.
33 R. Kantharaj and A. M. Marconnet, *Nanoscale Microscale Thermophys. Eng.*, 2019, **23**, 128–156.
34 S. S. Shinde, N. K. Wagh, S.-H. Kim and J.-H. Lee, *Adv. Sci.*, 2023, **10**, 2304235.
35 Y. Xiao, Y. Wang, S.-H. Bo, J. C. Kim, L. J. Miara and G. Ceder, *Nat. Rev. Mater.*, 2020, **5**, 105–126.
36 H. Chung and B. Kang, *Chem. Mater.*, 2017, **29**, 8611–8619.
37 J. Yan, D. Zhu, H. Ye, H. Sun, X. Zhang, J. Yao, J. Chen, L. Geng, Y. Su, P. Zhang, Q. Dai, Z. Wang, J. Wang, J. Zhao, Z. Rong, H. Li, B. Guo, S. Ichikawa, D. Gao, L. Zhang, J. Huang and Y. Tang, *ACS Energy Lett.*, 2022, **7**, 3855–3863.
38 K. Nie, X. Wang, J. Qiu, Y. Wang, Q. Yang, J. Xu, X. Yu, H. Li, X. Huang and L. Chen, *ACS Energy Lett.*, 2020, **5**, 826–832.
39 L. Wang, Z. Chen, Y. Liu, Y. Li, H. Zhang and X. He, *eTransportation*, 2023, **16**, 100239.
40 P. Lv, S. Xie, Q. Sun, X. Chen and Y. He, *ACS Appl. Energy Mater.*, 2022, **5**, 7199–7209.
41 M. Otoyama, A. Sakuda, M. Tatsumisago and A. Hayashi, *ACS Appl. Mater. Interfaces*, 2020, **12**, 29228–29234.
42 S.-J. Yang, J.-K. Hu, F.-N. Jiang, X.-B. Cheng, S. Sun, H.-J. Hsu, D. Ren, C.-Z. Zhao, H. Yuan, M. Ouyang, L.-Z. Fan, J.-Q. Huang and Q. Zhang, *eTransportation*, 2023, **18**, 100279.

43 T. Kim, K. Kim, S. Lee, G. Song, M. S. Jung and K. T. Lee, *Chem. Mater.*, 2022, **34**, 9159–9171.
44 G. Jia, Z. Deng, D. Ni, Z. Ji, D. Chen, X. Zhang, T. Wang, S. Li and Y. Zhao, *Front. Chem.*, 2022, **10**, 952875.
45 Y. Xiao, Y. Wang, S.-H. Bo, J. C. Kim, L. J. Miara and G. Ceder, *Nat. Rev. Mater.*, 2019, **5**, 105–126.
46 S. Kim, H. Oguchi, N. Toyama, T. Sato, S. Takagi, T. Otomo, D. Arunkumar, N. Kuwata, J. Kawamura and S. I. Orimo, *Nat. Commun.*, 2019, **10**, 1081.
47 Z. Lu and F. Ciucci, *Chem. Mater.*, 2017, **29**, 9308–9319.
48 T. Famprikis, P. Canepa, J. A. Dawson, M. S. Islam and C. Masquelier, *Nat. Mater.*, 2019, **18**, 1278–1291.
49 X. Liu, R. Garcia-Mendez, A. R. Lupini, Y. Cheng, Z. D. Hood, F. Han, A. Sharafi, J. C. Idrobo, N. J. Dudney, C. Wang, C. Ma, J. Sakamoto and M. Chi, *Nat. Mater.*, 2021, **20**, 1485–1490.
50 R. Chen, C. Yao, Q. Yang, H. Pan, X. Yu, K. Zhang and H. Li, *ACS Appl. Mater. Interfaces*, 2021, **13**, 18743–18749.
51 J. Mao, C. Ye, S. Zhang, F. Xie, R. Zeng, K. Davey, Z. Guo and S. Qiao, *Energy Environ. Sci.*, 2022, **15**, 2732–2752.
52 B. S. Vishnugopi, M. T. Hasan, H. Zhou and P. P. Mukherjee, *ACS Energy Lett.*, 2022, **8**, 398–407.
53 Y. Zhu and Y. Mo, *Angew. Chem., Int. Ed.*, 2020, **59**, 17472–17476.
54 Y. Li, J. Cheng, J. Li, Z. Zeng, Y. Guo, H. Zhang, H. Liu, X. Xu, Y. Rao, D. Li and L. Ci, *J. Power Sources*, 2022, **542**, 231794.
55 H. Liu, Q. Zhu, Y. Liang, C. Wang, D. Li, X. Zhao, L. Gao and L.-Z. Fan, *Chem. Eng. J.*, 2023, **462**, 142183.
56 F. Zhao, S. H. Alahakoon, K. Adair, S. Zhang, W. Xia, W. Li, C. Yu, R. Feng, Y. Hu, J. Liang, X. Lin, Y. Zhao, X. Yang, T. K. Sham, H. Huang, L. Zhang, S. Zhao, S. Lu, Y. Huang and X. Sun, *Adv. Mater.*, 2021, **33**, e2006577.
57 J. Liang, N. Chen, X. Li, X. Li, K. R. Adair, J. Li, C. Wang, C. Yu, M. Norouzi Banis, L. Zhang, S. Zhao, S. Lu, H. Huang, R. Li, Y. Huang and X. Sun, *Chem. Mater.*, 2020, **32**, 2664–2672.
58 G.-R. Zhu, Q. Zhang, Q.-S. Liu, Q.-Y. Bai, Y.-Z. Quan, Y. Gao, G. Wu and Y.-Z. Wang, *Nat. Commun.*, 2023, **14**, 4617.
59 F. N. Jiang, X. B. Cheng, S. J. Yang, J. Xie, H. Yuan, L. Liu, J. Q. Huang and Q. Zhang, *Adv. Mater.*, 2023, **35**, 2209114.
60 C. Wang, J. Liang, J. T. Kim and X. Sun, *Sci. Adv.*, 2022, **8**, eadc9516.
61 X. Li, J. Liang, N. Chen, J. Luo, K. R. Adair, C. Wang, M. N. Banis, T.-K. Sham, L. Zhang, S. Zhao, S. Lu, H. Huang, R. Li and X. Sun, *Angew. Chem., Int. Ed.*, 2019, **58**, 16427–16432.
62 X. Chen, Z. Jia, H. Lv, C. Wang, N. Zhao and X. Guo, *J. Power Sources*, 2022, **545**, 231939.
63 S. Wang, X. Xu, C. Cui, C. Zeng, J. Liang, J. Fu, R. Zhang, T. Zhai and H. Li, *Adv. Funct. Mater.*, 2021, **32**, 2108805.
64 W. D. Jung, M. Jeon, S. S. Shin, J.-S. Kim, H.-G. Jung, B.-K. Kim, J.-H. Lee, Y.-C. Chung and H. Kim, *ACS Omega*, 2020, **5**, 26015–26022.
65 X. Lu, Y. Wang, X. Xu, B. Yan, T. Wu and L. Lu, *Adv. Energy Mater.*, 2023, **13**, 2301746.
66 L.-Z. Fan, H. He and C.-W. Nan, *Nat. Rev. Mater.*, 2021, **6**, 1003–1019.
67 Y.-N. Liu, Z. Xiao, W.-K. Zhang, J. Zhang, H. Huang, Y.-P. Gan, X.-P. He, G. G. Kumar and Y. Xia, *Rare Met.*, 2022, **41**, 3762–3773.
68 Q. Liang, L. Chen, J. Tang, X. Liu, J. Liu, M. Tang and Z. Wang, *Energy Storage Mater.*, 2023, **55**, 847–856.
69 Z. Cui, E. Drioli and Y. M. Lee, *Prog. Polym. Sci.*, 2014, **39**, 164–198.
70 S. Zhang, Z. Li, Y. Guo, L. Cai, P. Manikandan, K. Zhao, Y. Li and V. G. Pol, *Chem. Eng. J.*, 2020, **400**, 125996.
71 L. Han, L. Wang, Z. Chen, Y. Kan, Y. Hu, H. Zhang and X. He, *Adv. Funct. Mater.*, 2023, **33**, 2300892.
72 J. Wan, J. Xie, X. Kong, Z. Liu, K. Liu, F. Shi, A. Pei, H. Chen, W. Chen, J. Chen, X. Zhang, L. Zong, J. Wang, L.-Q. Chen, J. Qin and Y. Cui, *Nat. Nanotechnol.*, 2019, **14**, 705–711.
73 Y. Cui, J. Wan, Y. Ye, K. Liu, L. Y. Chou and Y. Cui, *Nano Lett.*, 2020, **20**, 1686–1692.
74 W. Tang, S. Tang, C. Zhang, Q. Ma, Q. Xiang, Y.-W. Yang and J. Luo, *Adv. Energy Mater.*, 2018, **8**, 1800866.
75 D. Cai, D. Wang, Y. Chen, S. Zhang, X. Wang, X. Xia and J. Tu, *Chem. Eng. J.*, 2020, **394**, 124993.
76 P. Shi, J. Ma, M. Liu, S. Guo, Y. Huang, S. Wang, L. Zhang, L. Chen, K. Yang, X. Liu, Y. Li, X. An, D. Zhang, X. Cheng, Q. Li, W. Lv, G. Zhong, Y.-B. He and F. Kang, *Nat. Nanotechnol.*, 2023, **18**, 602–610.
77 Z. Wu, Z. Xie, J. Wang, T. Yu, X. Du, Z. Wang, X. Hao, A. Abudula and G. Guan, *Int. J. Hydrogen Energy*, 2020, **45**, 19601–19610.
78 S. H.-S. Cheng, K.-Q. He, Y. Liu, J.-W. Zha, M. Kamruzzaman, R. L.-W. Ma, Z.-M. Dang, R. K. Y. Li and C. Y. Chung, *Electrochim. Acta*, 2017, **253**, 430–438.
79 K. Deng, Q. Zeng, D. Wang, Z. Liu, G. Wang, Z. Qiu, Y. Zhang, M. Xiao and Y. Meng, *Energy Storage Mater.*, 2020, **32**, 425–447.
80 J. Zhao, M. Li, H. Su, Y. Liu, P. Bai, H. Liu, L. Ma, W. Li, J. Sun and Y. Xu, *Small Methods*, 2023, **7**, 2300228.
81 H. Duan, C. Wang, R. Yu, W. Li, J. Fu, X. Yang, X. Lin, M. Zheng, X. Li, S. Deng, X. Hao, R. Li, J. Wang, H. Huang and X. Sun, *Adv. Energy Mater.*, 2023, **13**, 2300815.
82 X. Fu, H. Duan, L. Zhang, Y. Hu and Y. Deng, *Adv. Funct. Mater.*, 2023, **33**, 2308022.
83 L. Hu, J. Wang, K. Wang, Z. Gu, Z. Xi, H. Li, F. Chen, Y. Wang, Z. Li and C. Ma, *Nat. Commun.*, 2023, **14**, 3807.
84 H. Pan, M. Zhang, Z. Cheng, H. Jiang, J. Yang, P. Wang, P. He and H. Zhou, *Sci. Adv.*, 2022, **8**, eabn4372.
85 J. Yu, Q. Liu, X. Hu, S. Wang, J. Wu, B. Liang, C. Han, F. Kang and B. Li, *Energy Storage Mater.*, 2022, **46**, 68–75.
86 X. Yang, M. Jiang, X. Gao, D. Bao, Q. Sun, N. Holmes, H. Duan, S. Mukherjee, K. Adair, C. Zhao, J. Liang, W. Li, J. Li, Y. Liu, H. Huang, L. Zhang, S. Lu, Q. Lu, R. Li, C. V. Singh and X. Sun, *Energy Environ. Sci.*, 2020, **13**, 1318–1325.
87 Q. Ruan, M. Yao, J. Lu, Y. Wang, J. Kong, H. Zhang and S. Zhang, *Energy Storage Mater.*, 2023, **54**, 294–303.

88 X. Yang, Q. Yin, C. Wang, K. Doyle-Davis, X. Sun and X. Li, *Prog. Mater. Sci.*, 2023, **140**, 101193.
89 M. Cai, Y. Dong, M. Xie, W. Dong, C. Dong, P. Dai, H. Zhang, X. Wang, X. Sun, S. Zhang, M. Yoon, H. Xu, Y. Ge, J. Li and F. Huang, *Nat. Energy*, 2023, **8**, 159–168.
90 S. Lee, K.-S. Lee, S. Kim, K. Yoon, S. Han, M. H. Lee, Y. Ko, J. H. Noh, W. Kim and K. Kang, *Sci. Adv.*, 2022, **8**, eabq0153.
91 Y. Chen, J. Qian, X. Hu, Y. Ma, Y. Li, T. Xue, T. Yu, L. Li, F. Wu and R. Chen, *Adv. Mater.*, 2023, **35**, 2212096.
92 H. Wan, Z. Wang, W. Zhang, X. He and C. Wang, *Nature*, 2023, **623**, 739–744.
93 W. Zhou, S. Wang, Y. Li, S. Xin, A. Manthiram and J. B. Goodenough, *J. Am. Chem. Soc.*, 2016, **138**, 9385–9388.
94 W. Kong, Z. Jiang, Y. Liu, Q. Han, L.-X. Ding, S. Wang and H. Wang, *Adv. Funct. Mater.*, 2023, **33**, 2306748.
95 C. Wang, K. Adair, J. Liang, X. Li, Y. Sun, X. Li, J. Wang, Q. Sun, F. Zhao, X. Lin, R. Li, H. Huang, L. Zhang, R. Yang, S.-G. Lu and X. Sun, *Adv. Funct. Mater.*, 2019, **29**, 1900392.
96 D. Lin, W. Liu, Y. Liu, H. R. Lee, P.-C. Hsu, K. Liu and Y. Cui, *Nano Lett.*, 2016, **16**, 459–465.
97 Q. Zhou, J. Ma, S. Dong, X. Li and G. Cui, *Adv. Mater.*, 2019, **31**, 1902029.
98 S. Choudhury, Z. Tu, A. Nijamudheen, M. J. Zachman, S. Stalin, Y. Deng, Q. Zhao, D. Vu, L. F. Kourkoutis, J. L. Mendoza-Cortes and L. A. Archer, *Nat. Commun.*, 2019, **10**, 3091.
99 S.-J. Yang, N. Yao, F.-N. Jiang, J. Xie, S.-Y. Sun, X. Chen, H. Yuan, X.-B. Cheng, J.-Q. Huang and Q. Zhang, *Angew. Chem., Int. Ed.*, 2022, **61**, e202214545.
100 H. Duan, M. Fan, W.-P. Chen, J.-Y. Li, P.-F. Wang, W.-P. Wang, J.-L. Shi, Y.-X. Yin, L.-J. Wan and Y.-G. Guo, *Adv. Mater.*, 2019, **31**, 1807789.
101 H. Xu, G. Cao, Y. Shen, Y. Yu, J. Hu, Z. Wang and G. Shao, *Energy Environ. Mater.*, 2022, **5**, 852–864.
102 K. Wang, Z. Liang, S. Weng, Y. Ding, Y. Su, Y. Wu, H. Zhong, A. Fu, Y. Sun, M. Luo, J. Yan, X. Wang and Y. Yang, *ACS Energy Lett.*, 2023, **8**, 3450–3459.
103 C. Liao, C. Yu, S. Chen, C. Wei, Z. Wu, S. Chen, Z. Jiang, S. Cheng and J. Xie, *Renewables*, 2023, **1**, 266–276.
104 F. Li, J. Li, F. Zhu, T. Liu, B. Xu, T.-H. Kim, M. J. Kramer, C. Ma, L. Zhou and C.-W. Nan, *Matter*, 2019, **1**, 1001–1016.
105 Z. Zhao, Z. Wen, X. Liu, H. Yang, S. Chen, C. Li, H. Lv, F. Wu, B. Wu and D. Mu, *Chem. Eng. J.*, 2021, **405**, 127031.
106 T. Yu, J. Liang, L. Luo, L. Wang, F. Zhao, G. Xu, X. Bai, R. Yang, S. Zhao, J. Wang, J. Yu and X. Sun, *Adv. Energy Mater.*, 2021, **11**, 2101915.
107 S. Zhang, F. Zhao, S. Wang, J. Liang, J. Wang, C. Wang, H. Zhang, K. Adair, W. Li, M. Li, H. Duan, Y. Zhao, R. Yu, R. Li, H. Huang, L. Zhang, S. Zhao, S. Lu, T.-K. Sham, Y. Mo and X. Sun, *Adv. Energy Mater.*, 2021, **11**, 2100836.
108 J. Wang, R. Chen, L. Yang, M. Zan, P. Chen, Y. Li, W. Li, H. Yu, X. Yu, X. Huang, L. Chen and H. Li, *Adv. Mater.*, 2022, **34**, 2200655.
109 J. Jiao, G. Lai, S. Qin, C. Fang, X. Xu, Y. Jiang, C. Ouyang and J. Zheng, *Acta Mater.*, 2022, **238**, 118229.
110 H.-J. Noh, S. Youn, C. S. Yoon and Y.-K. Sun, *J. Power Sources*, 2013, **233**, 121–130.
111 L. Geng, J. Liu, D. L. Wood, Y. F. Qin, W. Lu, C. J. Jafta, Y. Bai and I. Belharouak, *ACS Appl. Energy Mater.*, 2020, **3**, 7058–7065.
112 J.-N. Zhang, Q. Li, C. Ouyang, X. Yu, M. Ge, X. Huang, E. Hu, C. Ma, S. Li, R. Xiao, W. Yang, Y. Chu, Y. Liu, H. Yu, X.-Q. Yang, X. Huang, L. Chen and H. Li, *Nat. Energy*, 2019, **4**, 594–603.
113 L. Zou, J. Li, Z. Liu, G. Wang, A. Manthiram and C. Wang, *Nat. Commun.*, 2019, **10**, 3447.
114 R. Sim, Z. Cui and A. Manthiram, *ACS Energy Lett.*, 2023, **8**, 5143–5148.
115 H.-H. Ryu, H.-W. Lim, S. G. Lee and Y.-K. Sun, *Nat. Energy*, 2024, **9**, 47–56.
116 Y. Wang, Z. Wang, D. Wu, Q. Niu, P. Lu, T. Ma, Y. Su, L. Chen, H. Li and F. Wu, *eScience*, 2022, **2**, 537–545.
117 S. Sun, C.-Z. Zhao, H. Yuan, Z.-H. Fu, X. Chen, Y. Lu, Y.-F. Li, J.-K. Hu, J. Dong, J.-Q. Huang, M. Ouyang and Q. Zhang, *Sci. Adv.*, 2022, **8**, eadd5189.
118 X. Yang, X. Gao, M. Jiang, J. Luo, J. Yan, J. Fu, H. Duan, S. Zhao, Y. Tang, R. Yang, R. Li, J. Wang, H. Huang, X. Sun and C. V. Singh, *Angew. Chem., Int. Ed.*, 2023, **62**, e202215680.
119 T. Dai, S. Wu, Y. Lu, Y. Yang, Y. Liu, C. Chang, X. Rong, R. Xiao, J. Zhao, Y. Liu, W. Wang, L. Chen and Y.-S. Hu, *Nat. Energy*, 2023, **8**, 1221–1228.
120 F. Han, A. S. Westover, J. Yue, X. Fan, F. Wang, M. Chi, D. N. Leonard, N. J. Dudney, H. Wang and C. Wang, *Nat. Energy*, 2019, **4**, 187–196.
121 B. Shao, Y. Huang and F. Han, *Adv. Energy Mater.*, 2023, **13**, 2204098.
122 B. Jang, J. Woo, Y. B. Song, H. Kwak, J. Park, J. S. Kim, H. Lim and Y. S. Jung, *Energy Storage Mater.*, 2024, **65**, 103154.
123 H.-K. Tian, Z. Liu, Y. Ji, L.-Q. Chen and Y. Qi, *Chem. Mater.*, 2019, **31**, 7351–7359.
124 X. W. Chi, M. L. Li, J. C. Di, P. Bai, L. N. Song, X. X. Wang, F. Li, S. Liang, J. J. Xu and J. H. Yu, *Nature*, 2021, **592**, 551–557.
125 J.-M. Doux, H. Nguyen, D. H. S. Tan, A. Banerjee, X. Wang, E. A. Wu, C. Jo, H. Yang and Y. S. Meng, *Adv. Energy Mater.*, 2020, **10**, 1903253.
126 J. Sang, B. Tang, Y. Qiu, Y. Fang, K. Pan and Z. Zhou, *Energy Environ. Mater.*, 2024, e12670.
127 L. Qian, T. Or, Y. Zheng, M. Li, D. Karim, A. Cui, M. Ahmed, W. Park Hey, Z. Zhang, Y. Deng, A. Yu, Z. Chen and K. Amine, *Renewables*, 2023, **1**, 114–141.
128 S.-Y. Ham, H. Yang, O. Nunez-cuacuas, D. H. S. Tan, Y.-T. Chen, G. Deysher, A. Cronk, P. Ridley, J.-M. Doux, E. A. Wu, J. Jang and Y. S. Meng, *Energy Storage Mater.*, 2023, **55**, 455–462.
129 B. Lu, W. Bao, W. Yao, J.-M. Doux, C. Fang and Y. S. Meng, *J. Electrochem. Soc.*, 2022, **169**, 070537.
130 S. Zhang, F. Zhao, J. Chen, J. Fu, J. Luo, S. H. Alahakoon, L.-Y. Chang, R. Feng, M. Shakouri, J. Liang, Y. Zhao, X. Li, L. He, Y. Huang, T.-K. Sham and X. Sun, *Nat. Commun.*, 2023, **14**, 3780.

131 C. Zhu, T. Fuchs, S. A. L. Weber, F. H. Richter, G. Glasser, F. Weber, H.-J. Butt, J. Janek and R. Berger, *Nat. Commun.*, 2023, **14**, 1300.
132 Z. Ahmad, T. Xie, C. Maheshwari, J. C. Grossman and V. Viswanathan, *ACS Cent. Sci.*, 2018, **4**, 996–1006.
133 J. H. Cho, C. N. Im, C. H. Choi, S. H. Ha, H. K. Yoon, Y. Choi and J. Bae, *Electrochim. Acta*, 2020, **35**, 136612.
134 T. Inoue and K. Mukai, *ACS Appl. Mater. Interfaces*, 2017, **9**, 1507–1515.
135 X. Feng, M. Fang, X. He, M. Ouyang, L. Lu, H. Wang and M. Zhang, *J. Power Sources*, 2014, **255**, 294–301.
136 C. Wang, T. Deng, X. Fan, M. Zheng, R. Yu, Q. Lu, H. Duan, H. Huang, C. Wang and X. Sun, *Joule*, 2022, **6**, 1770–1781.
137 D. Cao, K. Zhang, W. Li, Y. Zhang, T. Ji, X. Zhao, E. Cakmak, J. Zhu, Y. Cao and H. Zhu, *Adv. Funct. Mater.*, 2023, **33**, 2307998.
138 C. Yuan, B. W. Sheldon and J. Xu, *Adv. Energy Mater.*, 2022, **12**, 2201804.
139 G. Lu, W. Liu, Z. Yang, Y. Wang, W. Zheng, R. Deng, R. Wang, L. Lu and C. Xu, *Adv. Funct. Mater.*, 2023, **33**, 2304407.
140 O. Furat, D. P. Finegan, Z. Yang, M. Neumann, S. Kim, T. R. Tanim, P. Weddle, K. Smith and V. Schmidt, *Energy Storage Mater.*, 2024, **64**, 103036.
141 T. M. M. Heenan, I. Mombrini, A. Llewellyn, S. Checchia, C. Tan, M. J. Johnson, A. Jnawali, G. Garbarino, R. Jervis, D. J. L. Brett, M. Di Michiel and P. R. Shearing, *Nature*, 2023, **617**, 507–512.
142 J.-P. Schmiegel, M. Leißing, F. Weddeling, F. Horsthemke, J. Reiter, Q. Fan, S. Nowak, M. Winter and T. Placke, *J. Electrochem. Soc.*, 2020, **167**, 060516.
143 J. Gu, X. Chen, R. Ma, Z. He, Z. Liang, H. Zhong, Y. Su, J. Shi and Y. Yang, *Energy Storage Mater.*, 2023, **63**, 103052.
144 X. Wu, G. Ji, J. Wang, G. Zhou and Z. Liang, *Adv. Mater.*, 2023, **35**, 2301540.
145 J. Fleming, T. Amietszajew, J. Charmet, A. J. Roberts, D. Greenwood and R. Bhagat, *J. Energy Storage*, 2019, **22**, 36–43.
146 D. P. Finegan, M. Scheel, J. B. Robinson, B. Tjaden, I. Hunt, T. J. Mason, J. Millichamp, M. Di Michiel, G. J. Offer, G. Hinds, D. J. L. Brett and P. R. Shearing, *Nat. Commun.*, 2015, **6**, 6924.
147 Y. Zhang, J. Feng, J. Qin, Y. L. Zhong, S. Zhang, H. Wang, J. Bell, Z. Guo and P. Song, *Adv. Sci.*, 2023, **10**, 2301056.
148 R. S. Longchamps, X.-G. Yang and C.-Y. Wang, *ACS Energy Lett.*, 2022, **7**, 1103–1111.
149 J. Deng, X. Li, C. Li, T. Wang, R. Liang, S. Li, Q. Huang and G. Zhang, *J. Energy Storage*, 2023, **72**, 108313.
150 X. Li, Q. Huang, J. Deng, G. Zhang, Z. Zhong and F. He, *J. Power Sources*, 2020, **451**, 227820.
151 Z. Rao, P. Lyu, P. Du, D. He, Y. Huo and C. Liu, *Battery Energy*, 2022, **1**, 20210019.
152 J. Gu, Z. Liang, J. Shi and Y. Yang, *Adv. Energy Mater.*, 2023, **13**, 2203153.
153 W. Mei, Z. Liu, C. Wang, C. Wu, Y. Liu, P. Liu, X. Xia, X. Xue, X. Han, J. Sun, G. Xiao, H.-Y. Tam, J. Albert, Q. Wang and T. Guo, *Nat. Commun.*, 2023, **14**, 5251.
154 P. Liu, L. Yang, B. Xiao, H. Wang, L. Li, S. Ye, Y. Li, X. Ren, X. Ouyang, J. Hu, F. Pan, Q. Zhang and J. Liu, *Adv. Funct. Mater.*, 2022, **32**, 2208586.
155 Y. Lv, X. Geng, W. Luo, T. Chu, H. Li, D. Liu, H. Cheng, J. Chen, X. He and C. Li, *J. Energy Storage*, 2023, **72**, 108389.
156 S. Yuan, C. Chang, S. Yan, P. Zhou, X. Qian, M. Yuan and K. Liu, *J. Energy Chem.*, 2021, **62**, 262–280.
157 Z. Jia, Y. Min, P. Qin, W. Mei, X. Meng, K. Jin, J. Sun and Q. Wang, *J. Energy Chem.*, 2024, **89**, 195–207.
158 X.-Q. Xu, X.-B. Cheng, F.-N. Jiang, S.-J. Yang, D. Ren, P. Shi, H. Hsu, H. Yuan, J.-Q. Huang, M. Ouyang and Q. Zhang, *SusMat*, 2022, **2**, 435–444.
159 M. Hu, Z. Tong, C. Cui, T. Zhai and H. Li, *Nano Lett.*, 2022, **22**, 3047–3053.
160 S.-J. Yang, N. Yao, X.-Q. Xu, F.-N. Jiang, X. Chen, H. Liu, H. Yuan, J.-Q. Huang and X.-B. Cheng, *J. Mater. Chem. A*, 2021, **9**, 19664–19668.
161 S.-J. Yang, F.-N. Jiang, J.-K. Hu, H. Yuan, X.-B. Cheng, S. Kaskel, Q. Zhang and J.-Q. Huang, *Electron*, 2023, **1**, e8.
162 Z. J. Baum, R. E. Bird, X. Yu and J. Ma, *ACS Energy Lett.*, 2022, **7**, 712–719.
163 G. Harper, R. Sommerville, E. Kendrick, L. Driscoll, P. Slater, R. Stolkin, A. Walton, P. Christensen, O. Heidrich, S. Lambert, A. Abbott, K. Ryder, L. Gaines and P. Anderson, *Nature*, 2019, **575**, 75–86.
164 X. Yu, W. Li, V. Gupta, H. Gao, D. Tran, S. Sarwar and Z. Chen, *Global Challenges*, 2022, **6**, 2200099.
165 L. Azhari, S. Bong, X. Ma and Y. Wang, *Matter*, 2020, **3**, 1845–1861.
166 D. H. Kim, D. Y. Oh, K. H. Park, Y. E. Choi, Y. J. Nam, H. A. Lee, S.-M. Lee and Y. S. Jung, *Nano Lett.*, 2017, **17**, 3013–3020.
167 A. Miura, N. C. Rosero-Navarro, A. Sakuda, K. Tadanaga, N. H. H. Phuc, A. Matsuda, N. Machida, A. Hayashi and M. Tatsumisago, *Nat. Rev. Chem.*, 2019, **3**, 189–198.
168 T. Yang, C. Wang, W. Zhang, Y. Xia, H. Huang, Y. Gan, X. He, X. Xia, X. Tao and J. Zhang, *J. Energy Chem.*, 2023, **84**, 189–209.
169 Y. Ishiguro, K. Ueno, S. Nishimura, G. Iida and Y. Igarashib, *Chem. Lett.*, 2023, **52**, 237–241.
170 H. Wan, B. Zhang, S. Liu, Z. Wang, J. Xu and C. Wang, *Adv. Energy Mater.*, 2024, **14**, 2303046.
171 Z. Wang, X. Lin, Y. Han, J. Cai, S. Wu, X. Yu and J. Li, *Nano Energy*, 2021, **89**, 106337.
172 Y. Xiao, Y. Wang, S.-H. Bo, J. C. Kim, L. Miara and G. Ceder, *Nat. Rev. Mater.*, 2020, **5**, 105–126.
173 S. Zhang, J. Ma, S. Dong and G. Cui, *Electrochem. Energy Rev.*, 2023, **6**, 4.
174 H. Liu, Y. Zhao, J. Zhou, P. Li, S.-H. Bo and S.-L. Chen, *ACS Appl. Energy Mater.*, 2020, **3**, 1260–1264.
175 J. Zhou, Y. Zhao, H. Liu, X. Tang, S.-L. Chen and S.-H. Bo, *J. Mater. Res.*, 2022, **37**, 3283–3296.
176 K. Liu, Z. Wei, C. Zhang, Y. Shang, R. Teodorescu and Q. L. Han, *IEEE/CAA J. Autom. Sin.*, 2022, **9**, 1139–1165.
177 J. Tian, R. Xiong, W. Shen, J. Lu and X.-G. Yang, *Joule*, 2021, **5**, 1521–1534.
178 L. Bravo Diaz, X. He, Z. Hu, F. Restuccia, M. Marinescu, J. V. Barreras, Y. Patel, G. Offer and G. Rein, *J. Electrochem. Soc.*, 2020, **167**, 090559.